

ChemMedChem

**Chemistry
Europe**
European Chemical
Societies Publishing

Accepted Article

Title: In Vitro and In Vivo Biological Evaluation of Novel 1,4-Naphthoquinone Derivatives as Potential Anticancer Agents

Authors: Ravichandiran Palanisamy, Aleksandra Martyna, Elżbieta Kochanowicz, Nikhil Maroli, Konrad Kubiński, Maciej Masłyk, Anna Boguszewska-Czubara, and Thiyagarajan Ramesh

This manuscript has been accepted after peer review and appears as an Accepted Article online prior to editing, proofing, and formal publication of the final Version of Record (VoR). The VoR will be published online in Early View as soon as possible and may be different to this Accepted Article as a result of editing. Readers should obtain the VoR from the journal website shown below when it is published to ensure accuracy of information. The authors are responsible for the content of this Accepted Article.

To be cited as: *ChemMedChem* **2024**, e202400495

Link to VoR: <https://doi.org/10.1002/cmdc.202400495>

WILEY-VCH

***In Vitro* and *In Vivo* Biological Evaluation of Novel 1,4-Naphthoquinone Derivatives as Potential Anticancer Agents**

Palanisamy Ravichandiran,^{1,2,7,*} Aleksandra Martyna,³ Elżbieta Kochanowicz,³ Nikhil Maroli,⁴ Konrad Kubiński,³ Maciej Masłyk,³ Anna Boguszevska-Czubara,⁵ and Thiyagarajan Ramesh⁶

¹ R&D Education Center for Whole Life Cycle R&D of Fuel Cell Systems, Jeonbuk National University, Jeonju, Jeollabuk-do 54896, Republic of Korea

² Department of Life Science, Department of Energy Storage/Conversion Engineering of Graduate School, Hydrogen and Fuel Cell Research Center, Jeonbuk National University, Jeonju, Jeollabuk-do 54896, Republic of Korea

³ Department of Molecular Biology, Institute of Biological Sciences, The John Paul II Catholic University of Lublin, ul. Konstantynów 1i, 20-708 Lublin, Poland

⁴ Department of Physics and Astronomy, University of Delaware, Newark, DE 19716, USA

⁵ Department of Medical Chemistry, Medical University of Lublin, Ul. Chodźki 4A, 20-093 Lublin, Poland

⁶ Department of Basic Medical Sciences, College of Medicine, Prince Sattam Bin Abdulaziz University, Al-Kharj 11942, Saudi Arabia

⁷ Present Address: Analytical, HP Green R & D Centre, Hindustan Petroleum Corporation Limited, KIADB Industrial Area, Devangundi, Hoskote, Bengaluru, 562114, Karnataka, India

*Corresponding author

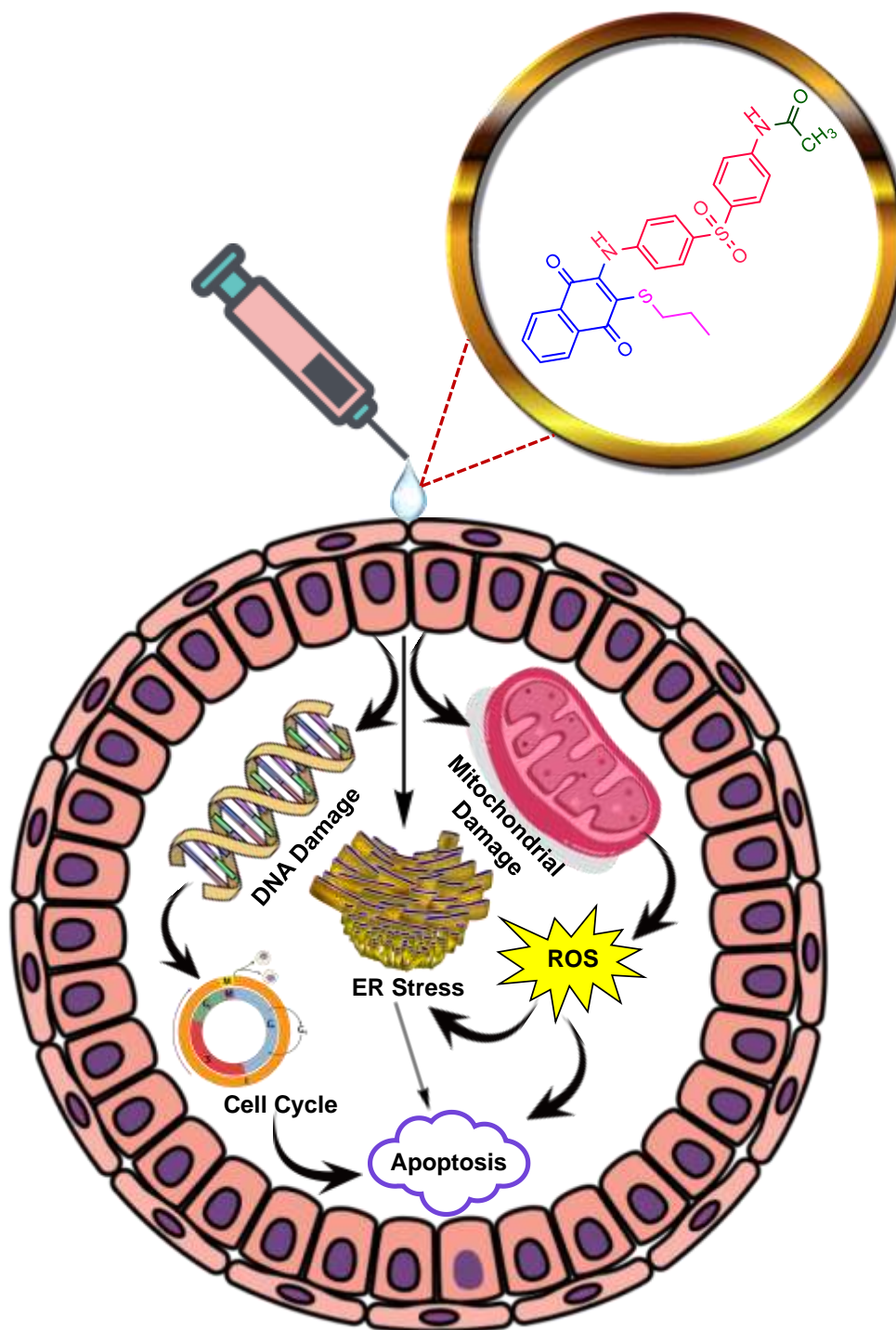
Dr. Palanisamy Ravichandiran

Department of Life Science, Department of Energy Storage/Conversion Engineering of Graduate School, Hydrogen and Fuel Cell Research Center, Jeonbuk National University, Jeonju, Jeollabuk-do 54896, Republic of Korea
Email: ravichandru55@gmail.com; Phone: +91-8870094922

Accepted Manuscript

Graphical Abstract

Compound **5v** exhibited superior anticancer properties compared to the other examined compounds. The compound's cytotoxicity was assessed in four different cancer carcinomas. The *in vivo* anticancer efficacy was evaluated through the xenograft of MCF-7 cells in zebrafish larvae.



Abstract

A novel library of naphthoquinone derivatives (**3–5aa**) was synthesized and evaluated for their anticancer properties. Specifically, compounds **5i**, **5l**, **5o**, **5q**, **5r**, **5s**, **5t**, and **5v** demonstrated superior cytotoxic activity against the cancer cell lines that were studied. All the studied compounds exhibited a higher selectivity index (SI) and a favourable safety profile than the standard drug doxorubicin. Notably, compound **5v** displayed a greater cytotoxic effect on MCF-7 cells ($IC_{50} = 1.2 \mu\text{M}$, and $0.9 \mu\text{M}$ at 24 h and 48 h, respectively) compared to the standard drug doxorubicin ($IC_{50} = 2.4 \mu\text{M}$, and $2.1 \mu\text{M}$ at 24 h and 48 h, respectively). To further investigate the mechanism of cytotoxic effect, additional anticancer studies were conducted with **5v** in MCF-7 cells. The studies are including morphological changes, AO/EB (acridine orange/ethidium bromide) double staining, apoptosis analysis, cell colony assay, SDS-PAGE and Western blotting, cell cycle analysis, and detecting reactive oxygen species (ROS) assay. The findings showed that **5v** triggered cytotoxic effects in MCF-7 cells through the initiation of cell cycle arrest at the G1/S phase and necrosis. *In vivo* ecotoxicity studies indicated that **5v** had lower toxicity towards zebrafish larvae ($LC_{50} = 50.15 \mu\text{M}$) and had an insignificant impact on cardiac functions. *In vivo* xenotransplantation of MCF-7 cells in zebrafish larvae demonstrated a significant reduction in tumour volume in the xenograft. Approximately 95% of the zebrafish larvae with **5v** xenografts survived after 10 days of the treatment. Finally, a computational modelling study was conducted on four protein receptors, namely ER, EFGR, BRCA1, and VEGFR2. The findings highlight the importance of the aminonaphthoquinone moiety, amide linkage, and propyl thio moiety in enhancing the anticancer properties. **5v** exhibited superior drug-likeness features and docking scores (-9.1, -7.1, -8.9, and -10.9 kcal/mol) compared to doxorubicin (-7.2, -6.1, -6.9, and -7.3 kcal/mol) against ER, EFGR, BRCA1, and VEGFR2 receptors, respectively. Therefore, the notable antitumor effects of naphthoquinone derivatives (**3–5aa**) suggest that these molecular

frameworks may play a role in the development of promising anticancer agents for cancer treatment.

Keywords: Naphthoquinone, cytotoxicity, breast cancer, zebrafish, xenotransplantation.

1. Introduction

Cancer is a collection of illnesses distinguished by the unregulated proliferation and dissemination of irregular cells, potentially leading to fatality if not addressed.^[1] In 2020, cancer claimed the lives of ten million individuals, making it the second leading cause of death worldwide.^[2] By 2040, it is projected that the number of new cases will rise by approximately 1.5 times compared to 2020.^{[3],[4]} In the United States, the 2022 data indicated nearly 1,918,030 new cancer cases and 609,360 cancer-related deaths.^[5] In the meantime, in India, the projected count of cancer instances in 2022 stood at 14,61,427, with a projected surge of 12.8% by 2025.^[6] There are various methods of cancer treatment available, including chemotherapy, radiotherapy, hormone therapy, and surgical removal.^[7] It is common to combine radiotherapy with hormone therapy or chemotherapy. It is crucial to acknowledge that radiotherapy and the indiscriminate nature of the medications employed in cancer therapy have the potential to damage healthy cells and result in systemic toxic effects.^[8] Immunotherapies are employed in cancer treatment, although they are not as frequently used as chemotherapy, surgery, and radiotherapy. Chemotherapy is a commonly utilized cancer treatment that has proven effective in addressing different forms of cancer. Nonetheless, it often leads to unintended side effects, including harm to healthy cells.^[9] Consequently, there is a continuous demand for the development of efficient anticancer agents with minimal side effects. It is critical to prioritize the advancement of novel molecules that can effectively address these challenges. For example, studies have indicated that naphthoquinones exhibit promising antitumor properties and selectivity indexes, making them potential candidates as alternative treatments for cancer.^{[10],[11]}

In this particular scenario, natural products and their derivatives serve as a valuable resource for assessing their potential anticancer properties. Many molecules act as a defence mechanism against various threats, including pathogens and tumors.^{[12],[13],[14],[15],[16]} Due to their diverse structures, these molecules often exhibit unique mechanisms of action, making them a promising platform for the development of new anticancer agents. Among the notable anticancer agents, quinones stands out as a natural metabolite that can be found in plants, microorganisms, and marine organisms.^{[17],[18],[19]} Additionally, it is a main core of several approved anticancer drugs, such as anthracyclines like doxorubicin, daunorubicin, and non-anthracycline antibiotics like bleomycin and mitoxantrone.^[20] Nevertheless, these derivatives mark a significant advancement in the battle against cancer; however, their effectiveness is constrained by issues such as poor selectivity, notable side effects, and the emergence of resistance. Additionally, a significant limitation of target-based drug discovery (TDD) lies in the challenges associated with the identification and validation of druggable anticancer targets. This process necessitates evidence that drug candidates interacting with potential targets exhibit clear clinical therapeutic benefits in cancer treatment, while also avoiding unacceptable side effects. Achieving this is nearly unfeasible during the initial phases of TDD. For instance, doxorubicin's cardiotoxicity is a well-documented for its side effects.^{[21],[22]}

Quinones, specifically naphthoquinone and anthraquinone, are commonly found in natural and pharmaceutical active compounds. They have been shown to possess various pharmacological properties, such as antiviral,^[23] antibacterial,^{[24],[25],[26]} antimalarial,^[27] antitrypanosomal,^[28] and antitumor,^{[29],[30]} activities. Quinones are known to generate ROS during their transformation, leading to DNA damage in cancer cells and triggering apoptosis. Moreover, quinones can selectively attack tumor cells due to their dependence on NAD(P)H quinone dehydrogenase 1 (NQO1) enzyme, which is often overexpressed in cancer cells. Numerous anticancer drugs with quinone components, such as napabucasin (BBI-608),

sepantronium bromide (YM-155), lawsone, and lapachol, have been approved or are in the final stages of drug discovery (Fig. 1). Survivin, a constituent of the inhibitor of apoptosis (IAP) protein family that suppresses caspases and prevents cell death, is frequently overexpressed in many cancers and is linked to an adverse clinical outcome.^[31] Notably, the initial survivin inhibitor YM155 is notably a naphthoquinone compound. Hence, compounds containing a quinone structure are viewed as potential survivin inhibitors in cancer treatment, as they target ILF3/NF110 and produce ROS to trigger DNA damage, autophagy, and apoptosis.^[32]

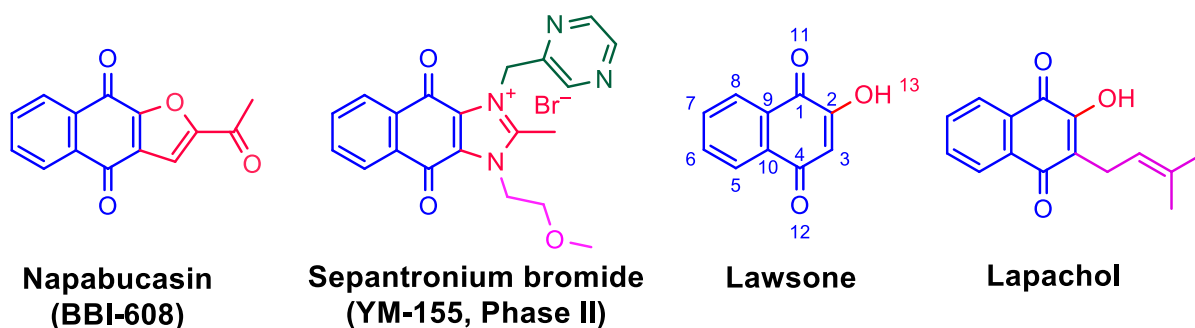


Fig. 1. Structures of 1,4-naphthoquinones used as an anticancer drug. Color representations: Red: C-2 substitution; Pink: C-3 substitution; Green: Extended conjugation.

Quinones exhibit a wide range of structural diversity. 1,4-Naphthoquinones are capable of accepting electrons in different biological systems, are frequently used as key components in the manufacturing of pharmaceutical drugs. Specifically, 1,4-naphthoquinones that have been altered at the C-2 position with a substituted amino group are seen as favorable choices for medical and biological applications.^{[33],[34],[35]} Aminonaphthoquinones play a crucial role in pharmacology.^{[36],[37],[38],[39]} At C-2 position, phenylamino moiety incorporation in 1,4-naphthoquinones has demonstrated an augmentation in their anticancer activities attributed to their redox potentials (compound I, Fig. 2).^{[40],[41]} Alkylamino derivatives demonstrate reduced anticancer efficacy in comparison to phenylamino naphthoquinones. Interestingly,

incorporating an acyl group into the phenylamino segment leads to heightened cytotoxicity effects, as seen in compound II.^[42] A recent research study highlighted the development of a promising anticancer agent by incorporating a sulfonamide group into phenylamino-1,4-naphthoquinone, which demonstrated inhibition of cell growth and induction of apoptosis (compound III) (Fig. 2).^[43]

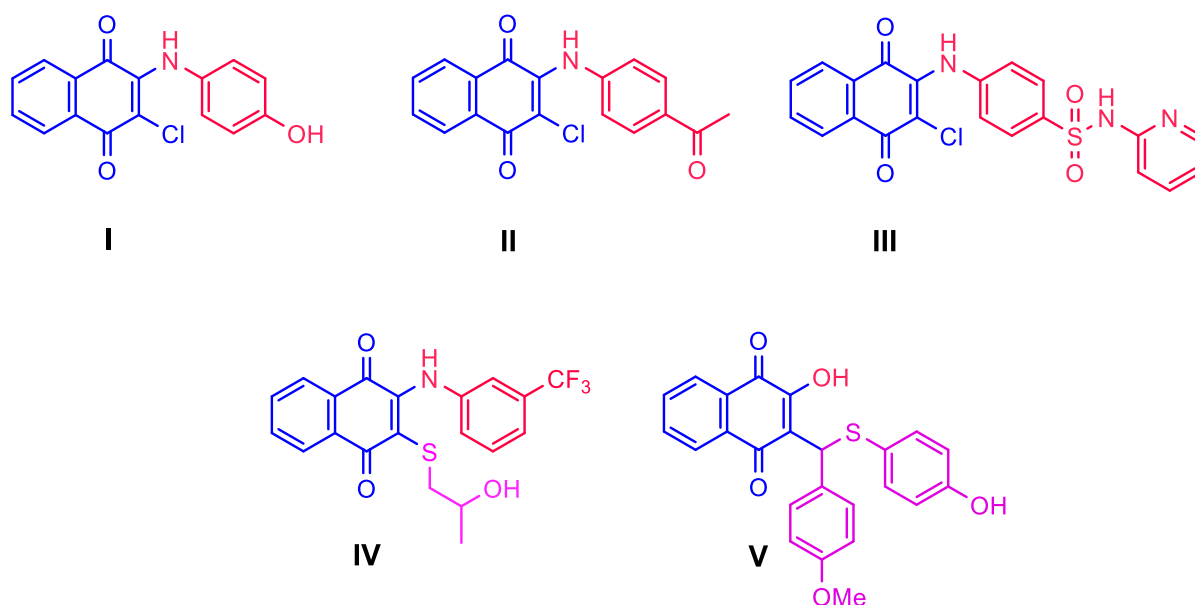


Fig. 2. Representative -N-, -S-, containing naphthoquinones exhibits intriguing biological activities.

New studies have shown that adding a thio group to the aminonaphthoquinone structure can greatly improve the bioactivity of the molecules. Yildirim et al. effectively showcased the preparation of a collection of 2,3-disubstituted-1,4-naphthoquinones with an arylamine and thiol groups, showing promising anticancer activities (compound IV).^[44] Dias et al. have synthesized aryl thiol-based naphthoquinones and evaluated its biological properties (compound V).^[45] However, the comprehensive *in vitro* and *in vivo* anticancer properties of 1,4-naphthoquinone with phenylamino-thio core in human cancer cell lines and animal models remains unexplored. (Fig. 2).

In our previous studies, we reported several libraries of naphthoquinones and evaluated their antimicrobial and anticancer properties.^{[46],[47],[26],[48]} In this current study, we are

introducing the synthesis of two new categories of naphthoquinones. These groups include phenylamino-thio-sulfone compounds with an acyl moiety as a counterpart (**3–5w**), as well as the corresponding phenylamino-thio-naphthoquinones (**5x–5aa**). As far as we know, these findings have not been reported in any existing literature. Furthermore, we conducted an assessment of the synthesized compounds (**3–5aa**) to determine their anticancer properties on four different cancer cell lines, as well as normal cells. Besides, a comprehensive investigation into the potential anticancer characteristics of the most active compound **5v** was conducted. This involved to study the morphological changes, AO/EB (acridine orange/ethidium bromide) double staining, apoptotic analysis, cell colony formation assay, SDS-PAGE and Western blotting, cell cycle analysis, and detecting reactive oxygen species (ROS) in MCF-7 cells. It is worth noting that the anticancer efficacy of **5v** was determined through *in vivo* xenotransplantation of MCF-7 cells in zebrafish larvae. To ensure the compound's safety, we also conducted ecotoxicity analysis to confirm its *in vivo* toxicity. Lastly, we employed *in silico* analysis to establish the binding modes and interaction mechanism of the compound **5v** with the cancer cell proteins.

2. Experimental Section

2.1. Chemistry

The melting points (°C) of all the synthesized compounds were determined using a melting point apparatus (Stuart, SMP10, Staffordshire, ST15 OSA, UK) in an open capillary tube. The chemicals and solvents used were purchased and directly used without any additional purification. Fourier-transform infrared spectroscopy analysis was conducted to characterize all the synthesized molecules (resolution of 0.4 cm^{-1} , ATR method, Perkin-Elmer, L1280135, Waltham, Massachusetts, USA). ^1H NMR and ^{13}C NMR spectroscopies were performed in DMSO- d_6 (500 MHz, Jeol, JNM-ECZ500S, 11 Dearborn Road Peabody, MA 01960, USA) and the J values are reported in Hz. The elemental analysis was conducted using a Flash 2000

Elemental Analyzer manufactured by Thermo Fisher Scientific Inc. in Waltham, Massachusetts, USA.

2.2. Synthesis of 2-((4-((4-aminophenyl)sulfonyl)phenyl)amino)-3-chloronaphthalene-1,4-dione (**3**)

As per our previously reported method, the compound **3** was synthesized^[49] with minor changes. 2,3-Dichloro-1,4-naphthoquinone **1** (2.270 g, 10 mmol) and dapsone **2** (2.048 g, 10 mmol) was added in a round bottomed flask, followed by the addition of double distilled water (900 mL). The reaction mixture was refluxed for 2 h. Upon completion of the reaction, the resulting deep red precipitate was filtered, washed with hot water (1000 mL), and dried at 40 °C. The crude product underwent purification *via* silica gel column chromatography (ethyl acetate: hexane, 1:2, 100–200 mesh) to yield compound **3** in the form of deep red crystals (88%); mp: 239–240 °C; IR (ATR): $\tilde{\nu}$ = 698, 1104, 1302, 1558, 1675, 3242, 3364, 3451. ¹H NMR (500 MHz, DMSO-*d*₆, 25 °C, TMS): δ = 6.18 (s, 2H, –NH₂), 6.62 (d, *J* = 10.90 Hz, 2H, Ar, sulfonyl moiety), 7.20 (d, *J* = 10.85 Hz, 2H, Ar, sulfonyl moiety), 7.54 (d, *J* = 10.90 Hz, 2H, Ar, sulfonyl moiety), 7.72 (d, *J* = 10.85 Hz, 2H, Ar, sulfonyl moiety), 7.81 (dt, *J* = 9.35 Hz & *J* = 1.55 Hz, 1H, Ar, quinone moiety), 7.87 (dt, *J* = 9.27 Hz & *J* = 1.05 Hz, 1H, Ar, quinone moiety), 8.04 (t, *J* = 7.40 Hz, 2H, Ar, quinone moiety), 9.52 (s, 1H, –NH) ppm. ¹³C NMR (125 MHz, DMSO-*d*₆): δ = 112.9, 119.0, 122.2, 125.9, 126.1, 126.6, 126.7, 129.2, 130.4, 131.6, 133.5, 134.6, 137.0, 142.5, 143.1, 153.4, 176.9 (–C = O, quinone moiety), 179.8 (–C = O, quinone moiety) ppm. Anal. calcd for C₂₂H₁₅ClN₂O₄S (438): C, 60.21; H, 3.45; N, 6.38; S, 7.30. Found: C, 60.33; H, 3.42; N, 6.42; S, 7.46; Beilstein test: Cl positive.^[50]

2.3. Synthesis of 2-((4-((4-aminophenyl)sulfonyl)phenyl)amino)-3-(propylthio)naphthalene-1,4-dione (**4**)

Compound **3** (1.75 g, 4 mmol) was dissolved in dry acetonitrile (400 mL), followed by the gradual addition of 1-propanethiol (0.371 g, 4 mmol) to the initial substance. The reaction

mixture was then supplemented with triethylamine (0.404 mL, 4 mmol) and refluxed for 3 h. Afterward, the reaction mixture was poured into ice-cold water, resulting in the formation of a solid product. This solid was subsequently filtered, dried at 50 °C, and subjected to purification through column chromatography (using silica gel, 100–200 mesh, ethyl acetate and hexane in a ratio of 1:2). The purification process yielded compound **4**, as a deep maroon solid (96%); mp: 155–156 °C; IR (ATR): $\tilde{\nu}$ = 702, 840, 1105, 1143, 1284, 1404, 1505, 1591, 1638, 2967, 3078, 3272, 3361, 3451. ¹H NMR (500 MHz, DMSO-*d*₆, 25 °C, TMS): δ = 0.67 (t, *J* = 9.05 Hz, 3H, –CH₃, propane thio moiety), 1.25 (q, *J* = 9.05 Hz, 2H, –CH₂, propane thio moiety), 2.54 (t, *J* = 8.95 Hz, 2H, –CH₂, propane thio moiety), 6.09 (s, 2H, –NH₂), 6.61 (d, *J* = 10.95 Hz, 2H, Ar, sulfonyl moiety), 7.10 (d, *J* = 10.90 Hz, 2H, Ar, sulfonyl moiety), 7.51 (d, *J* = 10.90 Hz, 2H, Ar, sulfonyl moiety), 7.68 (d, *J* = 10.90 Hz, 2H, Ar, sulfonyl moiety), 7.79 (dt, *J* = 9.22 Hz & *J* = 1.65 Hz, 1H, Ar, quinone moiety), 7.83 (dt, *J* = 9.12 Hz & *J* = 1.60 Hz, 1H, Ar, quinone moiety), 7.99 (t, *J* = 2.25 Hz, 1H, Ar, quinone moiety), 8.01 (t, *J* = 2.85 Hz, 1H, Ar, quinone moiety), 9.31 (s, 1H, –NH) ppm. ¹³C NMR (125 MHz, DMSO-*d*₆): δ = 12.9, 22.1, 34.5, 112.9, 120.4, 123.0, 126.1, 126.2, 126.8, 129.1, 130.7, 132.7, 133.4, 134.4, 135.7, 143.5, 144.1, 153.3, 179.7 (–C = O, quinone moiety), 180.7 (–C = O, quinone moiety) ppm. Anal. calcd for C₂₅H₂₂N₂O₄S₂ (478): C, 62.74; H, 4.63; N, 5.85; S, 13.40 Found: C, 62.61; H, 4.76; N, 5.99; S, 13.42.

2.4. Procedure for the synthesis of compounds **5a-5w**

The equal mole ratio of **4** (0.478 g, 1 mmol), and different varieties of acid chlorides (1 mmol) were thoroughly mixed in dry acetone (250 mL). The reaction mixture was refluxed for 30 min. The attained product mixture was transferred into ice-cold water. The solid was formed that was separated through a *vacuum* and dried at 40 °C. The crude product was purified by column chromatography (silica gel 100–200 mesh, ethyl acetate: hexane, 1:2) to afford clean samples of **5a-5w**.

2.4.1. *N*-(4-((4-((1,4-dioxo-3-(propylthio)-1,4-dihydronaphthalen-2-yl)amino)phenyl)sulfonyl)phenyl)benzamide (**5a**)

Violet solid (86%); mp: 210–211 °C; IR (ATR): $\tilde{\nu}$ = 739, 840, 1016, 1107, 1154, 1324, 1519, 1639, 1661, 1691, 2960, 3094, 3260, 3359. ¹H NMR (500 MHz, DMSO-*d*₆, 25 °C, TMS): δ = 0.65 (t, *J* = 9.10 Hz, 3H, –CH₃, propane thio moiety), 1.25 (q, *J* = 9.00 Hz, 2H, –CH₂, propane thio moiety), 2.54 (t, *J* = 8.95 Hz, 2H, –CH₂, propane thio moiety), 7.14 (d, *J* = 10.85 Hz, 2H, Ar, sulfonyl moiety), 7.53 (t, *J* = 8.90 Hz, 2H, Ar, sulfonyl moiety), 7.61 (t, *J* = 9.15 Hz, 1H, Ar, sulfonyl moiety), 7.78–7.81 (m, 3H, Ar, sulfonyl moiety), 7.84 (dd, *J* = 9.32 Hz & *J* = 1.75 Hz, 1H, Ar, quinone moiety), 7.91 (d, *J* = 11.00 Hz, 2H, Ar, quinone moiety), 7.95 (d, *J* = 9.15 Hz, 2H, Ar, quinone moiety), 7.99–8.03 (m, 4H, Ar, benzamide moiety), 9.38 (s, 1H, –NH), 10.61 (s, 1H, –NH) ppm. ¹³C NMR (125 MHz, DMSO-*d*₆): δ = 12.9, 22.1, 34.5, 120.1, 120.3, 124.0, 126.1, 126.2, 127.5, 127.5, 127.8, 128.2, 128.4, 130.7, 132.0, 132.6, 133.4, 133.7, 134.3, 135.9, 143.5, 143.7, 144.3, 166.0 (–C = O, benzamide moiety), 179.6 (–C = O, quinone moiety), 180.8 (–C = O, quinone moiety) ppm. Anal. calcd for C₃₂H₂₆N₂O₅S₂ (582): C, 65.96; H, 4.50; N, 4.81; S, 11.00 Found: C, 65.92; H, 4.57; N, 4.98; S, 11.30.

2.4.2. *N*-(4-((4-((1,4-dioxo-3-(propylthio)-1,4-dihydronaphthalen-2-yl)amino)phenyl)sulfonyl)phenyl)-2-fluorobenzamide (**5b**)

Deep Marron solid (92%); mp: 210–211 °C; IR (ATR): $\tilde{\nu}$ = 723, 837, 909, 1017, 1106, 1149, 1403, 1518, 1587, 1679, 3288, 3399 ¹H NMR (500 MHz, DMSO-*d*₆, 25 °C, TMS): δ = 0.65 (t, *J* = 9.15 Hz, 3H, –CH₃, propane thio moiety), 1.24 (q, *J* = 9.05 Hz, 2H, –CH₂, propane thio moiety), 2.53 (t, *J* = 8.90 Hz, 2H, –CH₂, propane thio moiety), 7.13 (d, *J* = 10.90 Hz, 2H, Ar, sulfonyl moiety), 7.34 (q, *J* = 9.90 Hz, 2H, Ar, sulfonyl moiety), 7.59 (t, *J* = 9.20 Hz, 1H, Ar, benzamide moiety), 7.66 (t, *J* = 8.10 Hz, 1H, Ar, benzamide moiety), 7.79 (d, *J* = 10.65 Hz, 3H, Ar, sulfonyl moiety), 7.84 (t, *J* = 8.10 Hz, 2H, Ar, sulfonyl moiety), 7.92 (s, 3H, Ar, quinone moiety), 8.00 (t, *J* = 8.40 Hz, 2H, Ar, quinone moiety), 9.43 (s, 1H, –NH), 10.85 (s,

1H, –NH) ppm. ¹³C NMR (125 MHz, DMSO-*d*₆): δ = 12.8, 22.1, 34.5, 116.0, 116.2, 199.7, 120.3, 124.1, 124.4, 124.5, 126.0, 126.2, 127.4, 128.2, 129.8, 130.7, 132.6, 132.8, 132.9, 133.3, 133.6, 134.2, 136.1, 143.0, 143.7, 144.3, 158.8 (d, *J* = 309.91 Hz), 163.2 (–C = O, benzamide moiety), 179.5 (–C = O, quinone moiety), 180.7 (–C = O, quinone moiety) ppm. ¹⁹F NMR (600 MHz, DMSO): δ = -114.3 ppm. Anal. calcd for C₃₂H₂₅FN₂O₅S₂ (600): C, 63.99; H, 4.20; N, 4.66; S, 10.67 Found: C, 63.82; H, 4.41; N, 4.90; S, 10.43.

2.4.3. *2-bromo-N-(4-((4-((1,4-dioxo-3-(propylthio)-1,4-dihydronaphthalen-2-yl)amino)phenyl)sulfonyl)phenyl)benzamide (5c)*

Light maroon solid (88%); mp: 227–228 °C; IR (ATR): $\tilde{\nu}$ = 719, 841, 1014, 1106, 1178, 1278, 1401, 1521, 1590, 1659, 1694, 2958, 3255, 3356. ¹H NMR (500 MHz, DMSO-*d*₆, 25 °C, TMS): δ = 0.65 (t, *J* = 9.15 Hz, 3H, –CH₃, propane thio moiety), 1.24 (q, *J* = 9.05 Hz, 2H, –CH₂, propane thio moiety), 2.54 (t, *J* = 8.85 Hz, 2H, –CH₂, propane thio moiety), 7.13 (d, *J* = 10.95 Hz, 2H, Ar, sulfonyl moiety), 7.43 (dt, *J* = 9.57 Hz & *J* = 2.10 Hz, 1H, Ar, quinone moiety), 7.50 (t, *J* = 9.15 Hz, 1H, Ar, quinone moiety), 7.56 (dd, *J* = 9.30 Hz & *J* = 2.10 Hz, 1H, Ar, quinone moiety), 7.72 (d, *J* = 9.80 Hz, 1H, Ar, quinone moiety), 7.78 (d, *J* = 10.90 Hz, 3H, Ar, sulfonyl moiety), 7.81–7.86 (m, 2H, Ar, sulfonyl moiety), 7.81 (t, *J* = 2.05 Hz, 1H, Ar, benzamide moiety), 7.84 (dd, *J* = 9.10 Hz & *J* = 1.65 Hz, 1H, Ar, benzamide moiety), 7.92 (s, 3H, Ar, benzamide moiety), 7.99–8.02 (m, 2H, Ar, sulfonyl moiety), 9.43 (s, 1H, –NH), 10.93 (s, 1H, –NH) ppm. ¹³C NMR (125 MHz, DMSO-*d*₆): δ = 12.9, 22.1, 34.5, 118.8, 119.6, 120.3, 124.1, 126.1, 126.3, 127.5, 127.7, 128.4, 128.8, 130.7, 131.5, 132.6, 132.7, 133.4, 133.6, 134.3, 136.2, 138.4, 143.1, 143.7, 144.4, 166.3 (–C = O, benzamide moiety), 179.6 (–C = O, quinone moiety), 180.8 (–C = O, quinone moiety) ppm. Anal. calcd for C₃₂H₂₅BrN₂O₅S₂ (661): C, 58.10; H, 3.81; N, 4.23; S, 9.69 Found: C, 58.32; H, 3.85; N, 4.41; S, 9.67.

2.4.4. *N-(4-((4-((1,4-dioxo-3-(propylthio)-1,4-dihydronaphthalen-2-yl)amino)phenyl)sulfonyl)phenyl)-3-(trifluoromethyl)benzamide (5d)*

Deep maroon solid (75%); mp: 197–198 °C; IR (ATR): $\tilde{\nu}$ = 688, 840, 910, 1015, 1105, 1149, 1283, 1401, 1519, 1590, 1665, 2966, 3315. ^1H NMR (500 MHz, DMSO- d_6 , 25 °C, TMS): δ = 0.64 (t, J = 9.15 Hz, 3H, $-\text{CH}_3$, propane thio moiety), 1.23 (q, J = 9.05 Hz, 2H, $-\text{CH}_2$, propane thio moiety), 2.53 (t, J = 8.85 Hz, 2H, $-\text{CH}_2$, propane thio moiety), 7.13 (d, J = 11.00 Hz, 2H, Ar, sulfonyl moiety), 7.80 (d, J = 10.65 Hz, 4H, Ar, sulfonyl moiety), 7.84 (dd, J = 9.20 Hz, J = 1.80 Hz, 1H, Ar, quinone moiety), 7.94 (d, J = 11.20 Hz, 2H, Ar, sulfonyl moiety), 7.98–8.02 (m, 5H, Ar, benzamide moiety), 8.26 (t, J = 9.35 Hz, 2H, Ar, quinone moiety), 9.44 (s, 1H, $-\text{NH}$), 10.83 (s, 1H, $-\text{NH}$) ppm. ^{13}C NMR (125 MHz, DMSO- d_6): δ = 12.8, 22.1, 34.5, 120.3, 124.1, 124.4, (d, J = 4.47 Hz), 125.2, 126.1, 126.2, 127.5, 128.2, 129.0 (q, J = 40.16 Hz), 129.8, 130.8, 132.0, 132.6, 133.4, 133.6, 134.3, 135.2, 136.3, 143.2, 143.7, 144.4, 164.6 ($-\text{C} = \text{O}$, benzamide moiety), 179.6 ($-\text{C} = \text{O}$, quinone moiety), 180.8 ($-\text{C} = \text{O}$, quinone moiety) ppm. ^{19}F NMR (600 MHz, DMSO): δ = -61.0 ppm. Anal. calcd for $\text{C}_{33}\text{H}_{25}\text{F}_3\text{N}_2\text{O}_5\text{S}_2$ (650): C, 60.91; H, 3.87; N, 4.31; S, 9.85 Found: C, 60.98; H, 3.80; N, 4.32; S, 9.98.

2.4.5. *3,5-dichloro-N-(4-((4-((1,4-dioxo-3-(propylthio)-1,4-dihydronaphthalen-2-yl)amino)phenyl)sulfonyl)phenyl)benzamide (5e)*

Deep maroon solid (84%); mp: 145–146 °C; IR (ATR): $\tilde{\nu}$ = 804, 1014, 1105, 1150, 1283, 1400, 1512, 1590, 1665, 2963, 3074, 3316. ^1H NMR (500 MHz, DMSO- d_6 , 25 °C, TMS): δ = 0.64 (t, J = 9.15 Hz, 3H, $-\text{CH}_3$, propane thio moiety), 1.24 (q, J = 9.10 Hz, 2H, $-\text{CH}_2$, propane thio moiety), 2.53 (t, J = 8.90 Hz, 2H, $-\text{CH}_2$, propane thio moiety), 7.13 (d, J = 10.95 Hz, 2H, Ar, sulfonyl moiety), 7.77–7.81 (m, 3H, Ar, sulfonyl moiety), 7.84 (dd, J = 8.92 Hz & J = 1.85 Hz, 1H, Ar, sulfonyl moiety), 7.87 (t, J = 2.25 Hz, 1H, Ar, quinone moiety), 7.92–7.94 (m, 2H, Ar, sulfonyl moiety), 7.96–7.97 (m, 3H, Ar, quinone moiety), 7.98–8.01 (m, 3H, Ar, benzamide moiety), 9.41 (s, 1H, $-\text{NH}$), 10.75 (s, 1H, $-\text{NH}$) ppm. ^{13}C NMR (125 MHz, DMSO- d_6): δ = 12.8, 22.1, 34.5, 120.3, 124.2, 126.1, 126.2, 126.6, 12.5, 128.2, 130.7, 131.3, 132.6, 133.4, 133.5, 134.3, 134.3, 136.4, 137.4, 142.9, 143.7, 144.4, 163.2 ($-\text{C} = \text{O}$, benzamide moiety),

179.6 (–C = O, quinone moiety), 180.8 (–C = O, quinone moiety) ppm. Anal. calcd for C₃₂H₂₄Cl₂N₂O₅S₂ (651): C, 58.99; H, 3.71; N, 4.30; S, 9.84 Found: C, 59.10; H, 3.82; N, 4.32; S, 9.80. Beilstein test: Cl positive.^[50]

2.4.6. *N*-(4-((4-((1,4-dioxo-3-(propylthio)-1,4-dihydronaphthalen-2-yl)amino)phenyl)sulfonyl)phenyl)-3,5-dinitrobenzamide (**5f**)

Deep maroon solid (98%); mp: 167–168 °C; IR (ATR): $\tilde{\nu}$ = 700, 719, 840, 1015, 1105, 1150, 1344, 1402, 1541, 1591, 1667, 3095, 3315. ¹H NMR (500 MHz, DMSO-*d*₆, 25 °C, TMS): δ = 0.65 (t, *J* = 9.15 Hz, 3H, –CH₃, propane thio moiety), 1.25 (q, *J* = 9.05 Hz, 2H, –CH₂, propane thio moiety), 2.54 (t, *J* = 8.85 Hz, 2H, –CH₂, propane thio moiety), 7.14 (d, *J* = 10.90 Hz, 2H, Ar, sulfonyl moiety), 7.79–7.81 (m, 3H, Ar, sulfonyl moiety), 7.84 (dd, *J* = 9.20 Hz & *J* = 1.70 Hz, 1H, Ar, sulfonyl moiety), 7.96–7.99 (m, 3H, Ar, sulfonyl moiety), 8.00–8.03 (m, 3H, Ar, quinone moiety), 9.01 (t, *J* = 2.45 Hz, 1H, Ar, quinone moiety), 9.15 (d, *J* = 2.55 Hz, 2H, Ar, benzamide moiety), 9.38 (s, 1H, –NH), 11.15 (s, 1H, –NH) ppm. ¹³C NMR (125 MHz, DMSO-*d*₆): δ = 12.8, 22.1, 34.5, 120.2, 120.6, 121.3, 124.3, 126.0, 126.6, 127.5, 128.1, 128.2, 130.7, 132.6, 133.4, 134.3, 136.8, 136.8, 142.5, 143.7, 144.4, 148.0, 161.8 (–C = O, benzamide moiety), 179.5 (–C = O, quinone moiety), 180.8 (–C = O, quinone moiety) ppm. Anal. calcd for C₃₂H₂₄N₄O₉S₂ (672): C, 57.14; H, 3.60; N, 8.33; S, 9.53 Found: C, 57.03; H, 3.91; N, 8.52; S, 9.41.

2.4.7. *N*-(4-((4-((1,4-dioxo-3-(propylthio)-1,4-dihydronaphthalen-2-yl)amino)phenyl)sulfonyl)phenyl)-3-nitrobenzamide (**5g**)

Deep maroon solid (99%); mp: 151–152 °C; IR (ATR): $\tilde{\nu}$ = 714, 836, 904, 1014, 1102, 1157, 1284, 1403, 1512, 1588, 1636, 1675, 2958, 3068, 3291, 3358. ¹H NMR (500 MHz, DMSO-*d*₆, 25 °C, TMS): δ = 0.65 (t, *J* = 9.10 Hz, 3H, –CH₃, propane thio moiety), 1.24 (q, *J* = 9.05 Hz, 2H, –CH₂, propane thio moiety), 2.53 (t, *J* = 8.90 Hz, 2H, –CH₂, propane thio moiety), 7.13 (d, *J* = 11.00 Hz, 2H, Ar, sulfonyl moiety), 7.79–7.81 (m, 3H, Ar, sulfonyl moiety), 7.83–7.86 (m,

2H, Ar, sulfonyl moiety), 7.94 (d, $J = 11.10$ Hz, 2H, Ar, sulfonyl moiety), 7.99–8.03 (m, 4H, Ar, quinone moiety), 8.38 (d, $J = 9.85$ Hz, 1H, Ar, benzamide moiety), 8.45 (dd, $J = 10.20$ Hz & $J = 2.00$ Hz, 1H, Ar, benzamide moiety), 8.78 (t, $J = 2.20$ Hz, 1H, Ar, benzamide moiety), 9.41 (s, 1H, –NH), 10.93 (s, 1H, –NH) ppm. ^{13}C NMR (125 MHz, DMSO- d_6): $\delta = 12.8, 22.1, 34.5, 120.3, 120.4, 122.5, 124.2, 126.1, 126.2, 126.5, 127.5, 128.2, 130.2, 130.7, 132.6, 133.4, 133.5, 134.3, 134.3, 135.6, 136.4, 143.0, 143.7, 144.4, 147.7, 163.9$ (–C = O, benzamide moiety), 179.6 (–C = O, quinone moiety), 180.8 (–C = O, quinone moiety) ppm. Anal. calcd for $\text{C}_{32}\text{H}_{25}\text{N}_3\text{O}_7\text{S}_2$ (627): C, 61.23; H, 4.01; N, 6.69; S, 10.22 Found: C, 61.03; H, 4.29; N, 6.65; S, 10.45.

2.4.8. *N*-(4-((4-((1,4-dioxo-3-(propylthio)-1,4-dihydronaphthalen-2-yl)amino)phenyl)sulfonyl)phenyl)-4-methyl-3-nitrobenzamide (**5h**)

Deep maroon solid (99%); mp: 141–142 °C; IR (ATR): $\tilde{\nu} = 836, 907, 1014, 1105, 1149, 1403, 1521, 1590, 1665, 2964, 3073, 3317$. ^1H NMR (500 MHz, DMSO- d_6 , 25 °C, TMS): $\delta = 0.64$ (t, $J = 9.10$ Hz, 3H, –CH₃, propane thio moiety), 1.24 (q, $J = 9.00$ Hz, 2H, –CH₂, propane thio moiety), 2.53 (t, $J = 8.95$ Hz, 2H, –CH₂, propane thio moiety), 2.59 (s, 3H, –CH₃, benzamide moiety), 7.13 (d, $J = 10.95$ Hz, 2H, Ar, sulfonyl moiety), 7.68 (d, $J = 10.15$ Hz, 1H, Ar, sulfonyl moiety), 7.78–7.81 (m, 3H, , Ar, benzamide moiety), 7.84 (dd, $J = 9.0$ Hz & $J = 1.40$ Hz, 1H, Ar, sulfonyl moiety), 8.56 (d, $J = 1.80$ Hz, 1H, Ar, quinone moiety), 9.40 (s, 1H, –NH), 10.80 (s, 1H, –NH) ppm. ^{13}C NMR (125 MHz, DMSO- d_6): $\delta = 12.8, 19.5, 22.1, 34.5, 120.3, 120.3, 123.6, 124.1, 126.0, 126.2, 127.5, 128.1, 130.7, 132.2, 132.6, 133.1, 133.4, 133.5, 134.3, 136.3, 136.7, 143.0, 143.7, 144.4, 148.7, 163.7$ (–C = O, benzamide moiety), 179.5 (–C = O, quinone moiety), 180.8 (–C = O, quinone moiety) ppm. Anal. calcd for $\text{C}_{33}\text{H}_{27}\text{N}_3\text{O}_7\text{S}_2$ (641): C, 61.77; H, 4.24; N, 6.55; S, 9.99 Found: C, 61.79; H, 4.31; N, 6.42; S, 9.97.

2.4.9. 4-chloro-*N*-(4-((4-((1,4-dioxo-3-(propylthio)-1,4-dihydronaphthalen-2-yl)amino)phenyl)sulfonyl)phenyl)-3-nitrobenzamide (**5i**)

Violet solid (95%); mp: 208–209 °C; IR (ATR): $\tilde{\nu}$ = 737, 837, 908, 1048, 1106, 1148, 1282, 1404, 1528, 1590, 1643, 2969, 3074, 3315. ¹H NMR (500 MHz, DMSO-*d*₆, 25 °C, TMS): δ = 0.64 (t, *J* = 9.15 Hz, 3H, –CH₃, propane thio moiety), 1.23 (q, *J* = 9.05 Hz, 2H, –CH₂, propane thio moiety), 2.53 (t, *J* = 8.90 Hz, 2H, –CH₂, propane thio moiety), 7.13 (d, *J* = 10.95 Hz, 2H, Ar, sulfonyl moiety), 7.78–7.82 (m, 3H, Ar, sulfonyl moiety), 7.84 (dd, *J* = 8.95 Hz & *J* = 1.70 Hz, 2H, , Ar, benzamide moiety), 7.95–7.98 (m, 4H, Ar, sulfonyl moiety), 7.99–8.01 (m, 3H, Ar, quinone moiety), 8.24 (dd, *J* = 10.55 Hz & *J* = 2.55 Hz, 1H, Ar, quinone moiety), 8.62 (d, *J* = 2.60 Hz, 1H, Ar, benzamide moiety), 9.41 (s, 1H, –NH), 10.88 (s, 1H, –NH) ppm. ¹³C NMR (125 MHz, DMSO-*d*₆): δ = 12.8, 22.1, 34.5, 120.3, 120.4, 124.2, 125.0, 126.1, 126.2, 127.5, 128.2, 128.5, 130.8, 132.0, 132.6, 132.9, 133.5, 133.5, 134.2, 136.5, 142.9, 143.7, 144.4, 147.3, 163.0 (–C = O, benzamide moiety), 179.6 (–C = O, quinone moiety), 180.8 (–C = O, quinone moiety) ppm. Anal. calcd for C₃₂H₂₄ClN₃O₇S₂ (662): C, 58.05; H, 3.65; N, 6.35; S, 9.68 Found: C, 58.39; H, 3.62; N, 6.12; S, 9.73. Beilstein test: Cl positive.^[50]

2.4.10. *N*-(4-((4-((1,4-dioxo-3-(propylthio)-1,4-dihydronaphthalen-2-yl)amino)phenyl)sulfonyl)phenyl)-4-methoxybenzamide (**5j**)

Deep maroon solid (87%); mp: 204–205 °C; IR (ATR): $\tilde{\nu}$ = 740, 1017, 1106, 1248, 1407, 1506, 1587, 1670, 3287, 3366. ¹H NMR (500 MHz, DMSO-*d*₆, 25 °C, TMS): δ = 0.68 (t, *J* = 9.05 Hz, 3H, –CH₃, propane thio moiety), 1.27 (q, *J* = 9.10 Hz, 2H, –CH₂, propane thio moiety), 2.57 (t, *J* = 8.65 Hz, 2H, –CH₂, propane thio moiety), 3.84 (s, 3H, –OCH₃, benzamide moiety), 7.06 (d, *J* = 9.50 Hz, 2H, Ar, sulfonyl moiety), 7.14 (d, *J* = 9.45 Hz, 2H, Ar, sulfonyl moiety), 7.77–7.83 (m, 4H, Ar, benzamide moiety), 7.88 (d, *J* = 9.55 Hz, 2H, Ar, sulfonyl moiety), 7.96 (d, *J* = 9.35 Hz, 2H, Ar, sulfonyl moiety), 8.00 (d, *J* = 9.15 Hz, 4H, Ar, quinone moiety), 9.25 (s, 1H, –NH), 10.37 (s, 1H, –NH) ppm. ¹³C NMR (125 MHz, DMSO-*d*₆): δ = 12.8, 22.0, 34.5, 55.4, 113.6, 119.9, 120.3, 124.0, 126.0, 126.2, 126.2, 127.4, 128.0, 129.7, 130.7, 132.6, 133.3, 133.7, 134.2, 135.5, 143.7, 144.3, 162.1 (–C = O, benzamide moiety), 179.5 (–C = O, quinone

moiety), 180.7 (–C = O, quinone moiety) ppm. Anal. calcd for C₃₃H₂₈N₂O₆S₂ (612): C, 64.69; H, 4.61; N, 4.57; S, 10.46 Found: C, 64.63; H, 4.85; N, 4.69; S, 10.42.

2.4.11. *N*-(4-((4-((1,4-dioxo-3-(propylthio)-1,4-dihydronaphthalen-2-yl)amino)phenyl)sulfonyl)phenyl)-4-methylbenzamide (**5k**)

Deep maroon solid (84%); mp: 209–210 °C; IR (ATR): $\tilde{\nu}$ = 717, 830, 1019, 1108, 1149, 1298, 1401, 1504, 1588, 1679, 2956, 3275. ¹H NMR (500 MHz, DMSO-*d*₆, 25 °C, TMS): δ = 0.64 (t, *J* = 9.10 Hz, 3H, –CH₃, propane thio moiety), 1.23 (q, *J* = 9.05 Hz, 2H, –CH₂, propane thio moiety), 2.37 (s, 3H, –CH₃, benzamide moiety), 2.53 (t, *J* = 8.95 Hz, 2H, –CH₂, propane thio moiety), 7.13 (d, *J* = 10.95 Hz, 2H, Ar, sulfonyl moiety), 7.34 (d, *J* = 10.20 Hz, 2H, Ar, sulfonyl moiety), 7.77–7.83 (m, 4H, Ar, benzamide moiety), 7.86 (d, *J* = 10.25 Hz, 2H, Ar, sulfonyl moiety), 7.90 (d, *J* = 11.05 Hz, 2H, Ar, sulfonyl moiety), 7.99–8.02 (m, 4H, Ar, quinone moiety), 9.40 (s, 1H, –NH), 10.53 (s, 1H, –NH) ppm. ¹³C NMR (125 MHz, DMSO-*d*₆): δ = 12.8, 21.0, 22.1, 34.5, 120.0, 120.3, 124.0, 126.0, 126.2, 127.4, 127.8, 128.1, 128.9, 130.7, 131.3, 132.6, 133.4, 133.7, 134.3, 135.7, 142.1, 143.6, 143.7, 144.3, 165.8 (–C = O, benzamide moiety), 179.5 (–C = O, quinone moiety), 180.8 (–C = O, quinone moiety) ppm. Anal. calcd for C₃₃H₂₈N₂O₅S₂ (596): C, 66.42; H, 4.73; N, 4.69; S, 10.75 Found: C, 66.32; H, 4.99; N, 4.65; S, 10.82.

2.4.12. 4-(*tert*-butyl)-*N*-(4-((4-((1,4-dioxo-3-(propylthio)-1,4-dihydronaphthalen-2-yl)amino)phenyl)sulfonyl)phenyl)benzamide (**5l**)

Blue violet solid (98%); mp: 223–224 °C; IR (ATR): $\tilde{\nu}$ = 692, 830, 1015, 1106, 1151, 1284, 1406, 1507, 1589, 1668, 2962, 3268, 3399. ¹H NMR (500 MHz, DMSO-*d*₆, 25 °C, TMS): δ = 0.64 (t, *J* = 9.05 Hz, 3H, –CH₃, propane thio moiety), 1.23 (q, *J* = 7.24 Hz, 2H, –CH₂, propane thio moiety), 1.28 (s, 3H, –CH₃, benzamide moiety), 1.30 (s, 6H, –CH₃, benzamide moiety), 2.53 (t, *J* = 8.85 Hz, 2H, –CH₂, propane thio moiety), 7.13 (d, *J* = 10.95 Hz, 2H, Ar, sulfonyl moiety), 7.55 (d, *J* = 10.55 Hz, 2H, Ar, sulfonyl moiety), 7.78–7.82 (m, 3H, Ar, sulfonyl

moiety), 7.86–7.92 (m, 5H, Ar, benzamide moiety), 8.00–8.02 (m, 4H, Ar, quinone moiety), 9.44 (s, 1H, –NH), 10.56 (s, 1H, –NH) ppm. ^{13}C NMR (125 MHz, DMSO- d_6): δ = 12.8, 22.1, 30.8, 34.5, 34.7, 120.0, 120.3, 124.0, 125.2, 125.3, 126.1, 126.2, 127.5, 127.7, 128.1, 129.1, 130.7, 131.6, 132.6, 133.4, 133.7, 134.3, 135.7, 143.6, 143.7, 144.3, 154.9, 166.0, 167.2 (–C = O, benzamide moiety), 179.6 (–C = O, quinone moiety), 180.8 (–C = O, quinone moiety) ppm. Anal. calcd for $\text{C}_{36}\text{H}_{34}\text{N}_2\text{O}_5\text{S}_2$ (638): C, 67.69; H, 5.37; N, 4.39; S, 10.04 Found: C, 67.78; H, 5.59; N, 4.72; S, 10.12.

2.4.13. *N*-(4-((4-((1,4-dioxo-3-(propylthio)-1,4-dihydronaphthalen-2-yl)amino)phenyl)sulfonyl)phenyl)-4-fluorobenzamide (**5m**)

Deep maroon solid (94%); mp: 196–197 °C; IR (ATR): $\tilde{\nu}$ = 722, 841, 1014, 1102, 1233, 1284, 1408, 1507, 1587, 1679, 2966, 3064, 3293, 3346. ^1H NMR (500 MHz, DMSO- d_6 , 25 °C, TMS): δ = 0.64 (t, J = 9.15 Hz, 3H, –CH₃, propane thio moiety), 1.23 (q, J = 9.05 Hz, 2H, –CH₂, propane thio moiety), 2.53 (t, J = 8.90 Hz, 2H, –CH₂, propane thio moiety), 7.13 (d, J = 10.85 Hz, 2H, Ar, sulfonyl moiety), 7.38 (t, J = 11.00 Hz, 2H, Ar, sulfonyl moiety), 7.78–7.85 (m, 4H, Ar, sulfonyl moiety), 7.92 (d, J = 10.95 Hz, 2H, Ar, quinone moiety), 7.99–8.05 (m, 6H, Ar, benzamide moiety), 9.43 (s, 1H, –NH), 10.64 (s, 1H, –NH) ppm. ^{13}C NMR (125 MHz, DMSO- d_6): δ = 12.9, 22.1, 34.5, 115.3, 115.5, 120.1, 120.3, 124.0, 126.1, 126.3, 127.5, 128.2, 130.6, 130.7, 130.7, 132.6, 133.4, 133.7, 134.3, 136.0, 143.5, 143.7, 144.3, 164.3 (d, J = 310.20 Hz), 164.9 (–C = O, benzamide moiety), 179.6 (–C = O, quinone moiety), 180.8 (–C = O, quinone moiety) ppm. ^{19}F NMR (600 MHz, DMSO): δ = -107.8 ppm. Anal. calcd for $\text{C}_{32}\text{H}_{25}\text{FN}_2\text{O}_5\text{S}_2$ (600): C, 63.99; H, 4.20; N, 4.66; S, 10.67 Found: C, 64.21; H, 4.51; N, 4.63; S, 10.39.

2.4.14. 4-chloro-*N*-(4-((4-((1,4-dioxo-3-(propylthio)-1,4-dihydronaphthalen-2-yl)amino)phenyl)sulfonyl)phenyl)benzamide (**5n**)

Deep maroon solid (99%); mp: 223–224 °C; IR (ATR): $\tilde{\nu}$ = 695, 744, 841, 1013, 1107, 1146, 1405, 1514, 1590, 1644, 1661, 1685, 2964, 3229. ¹H NMR (500 MHz, DMSO-*d*₆, 25 °C, TMS): δ = 0.64 (t, *J* = 9.15 Hz, 3H, –CH₃, propane thio moiety), 1.23 (q, *J* = 9.05 Hz, 2H, –CH₂, propane thio moiety), 2.52 (t, *J* = 8.90 Hz, 2H, –CH₂, propane thio moiety), 7.13 (d, *J* = 10.90 Hz, 2H, Ar, sulfonyl moiety), 7.61 (d, *J* = 10.70 Hz, 2H, Ar, sulfonyl moiety), 7.78–7.85 (m, 4H, Ar, sulfonyl moiety), 7.91–7.96 (m, 3H, Ar, quinone moiety), 7.98–8.01 (m, 5H, Ar, benzamide moiety), 9.43 (s, 1H, –NH), 10.69 (s, 1H, –NH) ppm. ¹³C NMR (125 MHz, DMSO-*d*₆): δ = 12.9, 22.1, 34.5, 120.2, 120.3, 124.0, 126.1, 126.3, 127.5, 128.2, 128.5, 129.8, 130.7, 132.6, 132.9, 133.4, 133.6, 134.3, 136.1, 136.9, 143.3, 143.7, 144.3, 164.9 (–C = O, benzamide moiety), 179.6 (–C = O, quinone moiety), 180.8 (–C = O, quinone moiety) ppm. Anal. calcd for C₃₂H₂₅ClN₂O₅S₂ (657): C, 62.28; H, 4.08; N, 4.54; S, 10.39 Found: C, 62.17; H, 4.31; N, 4.49; S, 10.68. Beilstein test: Cl positive.^[50]

2.4.15. 4-bromo-N-(4-((4-((1,4-dioxo-3-(propylthio)-1,4-dihydronaphthalen-2-yl)amino)phenyl)sulfonyl)phenyl)benzamide (5o)

Deep maroon solid (95%); mp: 235–236 °C; IR (ATR): $\tilde{\nu}$ = 694, 742, 842, 1010, 1147, 1286, 1407, 1514, 1589, 1684, 2967, 3230, 3403. ¹H NMR (500 MHz, DMSO-*d*₆, 25 °C, TMS): δ = 0.64 (t, *J* = 9.15 Hz, 3H, –CH₃, propane thio moiety), 1.23 (q, *J* = 9.05 Hz, 2H, –CH₂, propane thio moiety), 2.53 (t, *J* = 8.85 Hz, 2H, –CH₂, propane thio moiety), 7.13 (d, *J* = 10.95 Hz, 2H, Ar, sulfonyl moiety), 7.74–7.78 (m, 3H, Ar, sulfonyl moiety), 7.79–7.85 (m, 4H, Ar, sulfonyl moiety), 7.88–7.92 (m, 3H, Ar, quinone moiety), 7.98–8.01 (m, 4H, Ar, benzamide moiety), 9.40 (s, 1H, –NH), 10.67 (s, 1H, –NH) ppm. ¹³C NMR (125 MHz, DMSO-*d*₆): δ = 12.8, 22.1, 34.5, 120.2, 120.3, 124.1, 125.8, 126.0, 126.2, 127.5, 128.1, 129.9, 130.7, 131.4, 132.6, 133.3, 133.4, 133.6, 134.3, 136.1, 143.2, 143.7, 144.4, 165.0 (–C = O, benzamide moiety), 179.5 (–C = O, quinone moiety), 180.8 (–C = O, quinone moiety) ppm. Anal. calcd for C₃₂H₂₅BrN₂O₅S₂ (661): C, 58.10; H, 3.81; N, 4.23; S, 9.69 Found: C, 58.42; H, 3.92; N, 4.09; S, 9.70.

2.4.16. *N*-(4-((4-((1,4-dioxo-3-(propylthio)-1,4-dihydronaphthalen-2-yl)amino)phenyl)sulfonyl)phenyl)-4-nitrobenzamide (**5p**)

Light maroon solid (85%); mp: 215–216 °C; IR (ATR): $\tilde{\nu}$ = 692, 837, 1014, 1106, 1282, 1404, 1522, 1590, 1665, 2963, 3314. ¹H NMR (500 MHz, DMSO-*d*₆, 25 °C, TMS): δ = 0.64 (t, *J* = 9.10 Hz, 3H, –CH₃, propane thio moiety), 1.23 (q, *J* = 9.00 Hz, 2H, –CH₂, propane thio moiety), 2.53 (t, *J* = 8.75 Hz, 2H, –CH₂, propane thio moiety), 7.13 (d, *J* = 9.55 Hz, 2H, Ar, sulfonyl moiety), 7.79–7.85 (m, 4H, Ar, sulfonyl moiety), 7.94–8.02 (m, 6H, Ar, benzamide moiety), 8.17 (d, *J* = 9.45 Hz, 2H, Ar, sulfonyl moiety), 8.37 (d, *J* = 10.85 Hz, 2H, Ar, quinone moiety), 9.44 (s, 1H, –NH), 10.94 (s, 1H, –NH) ppm. ¹³C NMR (125 MHz, DMSO-*d*₆): δ = 13.3, 22.6, 35.1, 120.9, 121.0, 124.0, 124.6, 126.6, 126.8, 128.0, 128.7, 129.8, 131.1, 133.0, 134.0, 134.1, 134.9, 137.0, 140.4, 143.4, 144.2, 144.8, 149.8, 165.1 (–C = O, benzamide moiety), 180.1 (–C = O, quinone moiety), 181.4 (–C = O, quinone moiety) ppm. Anal. calcd for C₃₂H₂₅N₃O₇S₂ (627): C, 61.23; H, 4.01; N, 6.69; S, 10.22 Found: C, 61.48; H, 4.38; N, 6.61; S, 10.21.

2.4.17. *N*-(4-((4-((1,4-dioxo-3-(propylthio)-1,4-dihydronaphthalen-2-yl)amino)phenyl)sulfonyl)phenyl)furan-2-carboxamide (**5q**)

Violet solid (96%); mp: 214–215 °C; IR (ATR): $\tilde{\nu}$ = 740, 833, 1016, 1149, 1407, 1520, 1588, 1640, 1694, 2968, 3242, 3354. ¹H NMR (500 MHz, DMSO-*d*₆, 25 °C, TMS): δ = 0.64 (t, *J* = 9.10 Hz, 3H, –CH₃, propane thio moiety), 1.23 (q, *J* = 9.05 Hz, 2H, –CH₂, propane thio moiety), 2.53 (t, *J* = 8.90 Hz, 2H, –CH₂, propane thio moiety), 6.71 (q, *J* = 2.2 Hz, 1H, Ar, quinone moiety), 7.13 (d, *J* = 10.95 Hz, 2H, Ar, sulfonyl moiety), 7.39 (d, *J* = 4.35 Hz, 1H, Ar, quinone moiety), 7.78–7.85 (m, 4H, Ar, sulfonyl moiety), 7.89 (d, *J* = 4.35 Hz, 1H, Ar, sulfonyl moiety), 7.96–8.02 (m, 5H, Ar, benzamide moiety), 9.40 (s, 1H, –NH), 10.56 (s, 1H, –NH) ppm. ¹³C NMR (125 MHz, DMSO-*d*₆): δ = 12.8, 22.1, 34.5, 112.3, 115.7, 120.1, 120.3, 124.1, 126.0, 126.2, 127.5, 128.1, 130.7, 132.6, 133.4, 133.6, 134.3, 135.9, 142.9, 143.7, 144.3, 146.2, 146.8, 156.4 (–C = O, benzamide moiety), 179.5 (–C = O, quinone moiety), 180.8 (–C = O, quinone

moiety) ppm. Anal. calcd for C₃₀H₂₄N₂O₆S₂ (572): C, 62.92; H, 4.22; N, 4.89; S, 11.20 Found: C, 62.90; H, 4.48; N, 4.97; S, 11.46.

2.4.18. *N*-(4-((4-((1,4-dioxo-3-(propylthio)-1,4-dihydronaphthalen-2-yl)amino)phenyl)sulfonyl)phenyl)thiophene-2-carboxamide (**5r**)

Violet solid (98%); mp: 230–231 °C; IR (ATR): $\tilde{\nu}$ = 844, 905, 1015, 1106, 1285, 1409, 1526, 1585, 1671, 2970, 3244, 3350. ¹H NMR (500 MHz, DMSO-*d*₆, 25 °C, TMS): δ = 0.63 (t, *J* = 9.10 Hz, 3H, –CH₃, propane thio moiety), 1.23 (q, *J* = 9.10 Hz, 2H, –CH₂, propane thio moiety), 2.52 (t, *J* = 8.85 Hz, 2H, –CH₂, propane thio moiety), 7.13 (d, *J* = 10.90 Hz, 2H, Ar, sulfonyl moiety), 7.24 (t, *J* = 5.00 Hz, 1H, Ar, benzamide moiety), 7.78–7.85 (m, 4H, Ar, sulfonyl moiety), 7.90–7.79 (m, 5H, Ar, benzamide moiety), 7.99–8.02 (m, 2H, Ar, sulfonyl moiety), 8.05 (d, *J* = 4.65 Hz, 1H, Ar, quinone moiety), 9.44 (s, 1H, –NH), 10.58 (s, 1H, –NH) ppm. ¹³C NMR (125 MHz, DMSO-*d*₆): δ = 12.9, 22.1, 34.5, 120.0, 120.3, 124.0, 126.1, 126.3, 127.5, 128.2, 129.9, 130.7, 132.6, 132.7, 133.4, 133.6, 134.3, 135.9, 139.2, 143.2, 143.7, 144.3, 160.2 (–C = O, benzamide moiety), 179.6 (–C = O, quinone moiety), 180.8 (–C = O, quinone moiety) ppm. Anal. calcd for C₃₀H₂₄N₂O₅S₃ (588): C, 61.21; H, 4.11; N, 4.76; S, 16.34 Found: C, 61.13; H, 4.40; N, 4.61; S, 16.39.

2.4.19. 2-(4-chlorophenyl)-*N*-(4-((4-((1,4-dioxo-3-(propylthio)-1,4-dihydronaphthalen-2-yl)amino)phenyl)sulfonyl)phenyl)acetamide (**5s**)

Deep maroon solid (94%); mp: 125–126 °C; IR (ATR): $\tilde{\nu}$ = 716, 837, 1015, 1104, 1147, 1282, 1402, 1509, 1588, 1664, 2962, 3062, 3317. ¹H NMR (500 MHz, DMSO-*d*₆, 25 °C, TMS): δ = 0.62 (t, *J* = 9.10 Hz, 3H, –CH₃, propane thio moiety), 1.21 (q, *J* = 9.05 Hz, 2H, –CH₂, propane thio moiety), 2.51 (t, *J* = 8.90 Hz, 2H, –CH₂, propane thio moiety), 3.68 (s, 2H, –CH₂, acetamide moiety), 7.11 (d, *J* = 10.85 Hz, 2H, Ar, sulfonyl moiety), 7.34 (q, *J* = 14.35 Hz, 4H, Ar, sulfonyl moiety), 7.75–7.83 (m, 6H, Ar, benzamide moiety), 7.86 (d, *J* = 11.00 Hz, 2H, Ar, sulfonyl moiety), 7.99–8.01 (m, 2H, Ar, quinone moiety), 9.43 (s, 1H, –NH), 10.61 (s, 1H, –

NH) ppm. ^{13}C NMR (125 MHz, DMSO- d_6): δ = 13.3, 22.6, 35.0, 42.9, 119.6, 120.9, 124.7, 126.6, 126.8, 128.0, 128.7, 128.8, 131.3, 131.5, 131.9, 133.2, 133.9, 134.3, 134.9, 134.9, 136.1, 143.8, 144.3, 144.9, 170.0 (–C = O, benzamide moiety), 180.1 (–C = O, quinone moiety), 181.3 (–C = O, quinone moiety) ppm. Anal. calcd for $\text{C}_{33}\text{H}_{27}\text{ClN}_2\text{O}_5\text{S}_2$ (631): C, 62.80; H, 4.31; N, 4.44; S, 10.16 Found: C, 62.97; H, 4.48; N, 4.37; S, 10.48. Beilstein test: Cl positive.^[50]

2.4.20. *N*-(4-((4-((1,4-dioxo-3-(propylthio)-1,4-dihydronaphthalen-2-yl)amino)phenyl)sulfonyl)phenyl)-1-naphthamide (**5t**)

Orange solid (99%); mp: 224–225 °C; IR (ATR): $\tilde{\nu}$ = 697, 737, 831, 906, 1015, 1104, 1146, 1280, 1403, 1511, 1588, 1663, 2957, 3231, 3342. ^1H NMR (500 MHz, DMSO- d_6 , 25 °C, TMS): δ = 0.67 (t, J = 9.00 Hz, 3H, –CH₃, propane thio moiety), 1.26 (q, J = 8.90 Hz, 2H, –CH₂, propane thio moiety), 2.56 (t, J = 8.45 Hz, 2H, –CH₂, propane thio moiety), 7.15 (d, J = 10.30 Hz, 2H, Ar, sulfonyl moiety), 7.58–7.63 (m, 3H, Ar, sulfonyl moiety), 7.76–7.86 (m, 5H, Ar, quinone moiety), 7.95 (d, J = 10.80 Hz, 2H, Ar, sulfonyl moiety), 8.02–8.11 (m, 6H, Ar, benzamide moiety), 8.14–8.16 (m, 1H, Ar, benzamide moiety), 9.42 (s, 1H, –NH), 10.99 (s, 1H, –NH) ppm. ^{13}C NMR (125 MHz, DMSO- d_6): δ = 12.8, 22.1, 34.5, 119.7, 120.3, 124.1, 124.9, 124.9, 125.7, 126.0, 126.2, 126.4, 127.1, 127.5, 128.3, 128.3, 129.5, 130.5, 130.7, 132.6, 133.1, 133.4, 133.7, 133.9, 134.3, 136.0, 143.5, 143.8, 144.4, 167.7 (–C = O, benzamide moiety), 179.5 (–C = O, quinone moiety), 180.8 (–C = O, quinone moiety) ppm. Anal. calcd for $\text{C}_{36}\text{H}_{28}\text{N}_2\text{O}_5\text{S}_2$ (632): C, 68.34; H, 4.46; N, 4.43; S, 10.13 Found: C, 68.12; H, 4.63; N, 4.41; S, 10.48.

2.4.21. *N*-(4-((4-((1,4-dioxo-3-(propylthio)-1,4-dihydronaphthalen-2-yl)amino)phenyl)sulfonyl)phenyl)propionamide (**5u**)

Deep maroon solid (88%); mp: 179–180 °C; IR (ATR): $\tilde{\nu}$ = 837, 908, 1015, 1106, 1149, 1284, 1404, 1522, 1590, 1662, 2965, 3261, 3323. ^1H NMR (500 MHz, DMSO- d_6 , 25 °C, TMS): δ = 0.63 (t, J = 9.10 Hz, 3H, –CH₃, propane thio moiety), 1.06 (t, J = 9.30 Hz, 3H, –CH₃,

propionamide moiety), 1.23 (q, $J = 9.05$ Hz, 2H, $-\text{CH}_2$, propane thio moiety), 2.34 (q, $J = 9.50$ Hz, 2H, $-\text{CH}_3$, propionamide moiety), 2.53 (d, $J = 8.90$ Hz, 2H, $-\text{CH}_2$, propane thio moiety), 7.12 (d, $J = 10.95$ Hz, 2H, Ar, sulfonyl moiety), 7.75–7.80 (m, 4H, Ar, sulfonyl moiety), 7.81–7.86 (m, 4H, Ar, quinone moiety), 7.99–8.01 (m, 2H, Ar, sulfonyl moiety), 9.42 (s, 1H, $-\text{NH}$), 10.30 (s, 1H, $-\text{NH}$) ppm. ^{13}C NMR (125 MHz, $\text{DMSO}-d_6$): $\delta = 9.4, 12.8, 22.1, 29.6, 34.5, 118.8, 120.3, 123.9, 126.1, 126.2, 127.4, 128.3, 130.7, 132.6, 133.4, 133.8, 134.3, 135.1, 143.6, 143.7, 144.2, 172.7$ ($-\text{C} = \text{O}$, propionamide moiety), 179.6 ($-\text{C} = \text{O}$, quinone moiety), 180.8 ($-\text{C} = \text{O}$, quinone moiety) ppm. Anal. calcd for $\text{C}_{28}\text{H}_{26}\text{N}_2\text{O}_5\text{S}_2$ (534): C, 62.90; H, 4.90; N, 5.24; S, 11.99 Found: C, 62.89; H, 4.58; N, 5.01; S, 11.80.

2.4.22. *N*-(4-((4-((1,4-dioxo-3-(propylthio)-1,4-dihydronaphthalen-2-yl)amino)phenyl)sulfonyl)phenyl)furan-2-carboxamide (**5v**)

Deep maroon solid (75%); mp: 143–144 °C; IR (ATR): $\tilde{\nu} = 718, 842, 1016, 1106, 1146, 1295, 1403, 1515, 1589, 1663, 2962, 3310$. ^1H NMR (500 MHz, $\text{DMSO}-d_6$, 25 °C, TMS): $\delta = 0.63$ (t, $J = 9.10$ Hz, 3H, $-\text{CH}_3$, propane thio moiety), 1.23 (q, $J = 9.05$ Hz, 2H, $-\text{CH}_2$, propane thio moiety), 2.06 (s, 3H, $-\text{CH}_3$, carboxamide moiety), 2.53 (d, $J = 8.90$ Hz, 2H, $-\text{CH}_2$, propane thio moiety), 7.12 (d, $J = 10.95$ Hz, 2H, Ar, sulfonyl moiety), 7.75–7.79 (m, 4H, Ar, sulfonyl moiety), 7.81–7.85 (m, 4H, Ar, quinone moiety), 7.98–8.01 (m, 2H, Ar, sulfonyl moiety), 9.39 (s, 1H, $-\text{NH}$), 10.35 (s, 1H, $-\text{NH}$) ppm. ^{13}C NMR (125 MHz, $\text{DMSO}-d_6$): $\delta = 12.8, 22.1, 24.1, 34.5, 118.8, 120.3, 124.0, 126.1, 126.2, 127.4, 128.3, 130.7, 132.6, 133.4, 133.8, 134.3, 135.2, 143.5, 143.8, 144.3, 169.0$ ($-\text{C} = \text{O}$, carboxamide moiety), 179.6 ($-\text{C} = \text{O}$, quinone moiety), 180.8 ($-\text{C} = \text{O}$, quinone moiety) ppm. Anal. calcd for $\text{C}_{27}\text{H}_{24}\text{N}_2\text{O}_5\text{S}_2$ (520): C, 62.29; H, 4.65; N, 5.38; S, 12.32 Found: C, 62.03; H, 4.89; N, 5.42; S, 12.31.

2.4.23. 2,2-dichloro-*N*-(4-((4-((1,4-dioxo-3-(propylthio)-1,4-dihydronaphthalen-2-yl)amino)phenyl)sulfonyl)phenyl)acetamide (**5w**)

Deep maroon solid (93%); mp: 197–198 °C; IR (ATR): $\tilde{\nu}$ = 793, 837, 909, 1013, 1104, 1152, 1283, 1408, 1510, 1676, 1725, 2971, 3284. ^1H NMR (500 MHz, DMSO- d_6 , 25 °C, TMS): δ = 0.62 (t, J = 9.15 Hz, 3H, –CH₃, propane thio moiety), 1.22 (q, J = 9.00 Hz, 2H, –CH₂, propane thio moiety), 2.53 (t, J = 8.90 Hz, 2H, –CH₂, propane thio moiety), 6.60 (s, 1H, –CH, acetamide moiety), 7.12 (d, J = 10.95 Hz, 2H, Ar, sulfonyl moiety), 7.77–7.80 (m, 3H, Ar, sulfonyl moiety), 7.81–7.86 (m, 3H, Ar, sulfonyl moiety), 7.94 (d, J = 11.00 Hz, 2H, Ar, quinone moiety), 7.99–8.02 (m, 2H, Ar, quinone moiety), 9.44 (s, 1H, –NH), 11.07 (s, 1H, –NH) ppm. ^{13}C NMR (125 MHz, DMSO- d_6): δ = 13.3, 22.6, 35.0, 67.6, 120.6, 120.8, 124.9, 126.6, 126.8, 128.1, 129.0, 131.3, 133.2, 133.9, 134.0, 134.9, 137.7, 142.3, 144.2, 145.0, 162.8 (–C = O, acetamide moiety), 180.1 (–C = O, quinone moiety), 181.4 (–C = O, quinone moiety) ppm. Anal. calcd for C₂₇H₂₂Cl₂N₂O₅S₂ (589): C, 55.01; H, 3.76; N, 4.75; S, 10.80 Found: C, 55.27; H, 3.92; N, 4.78; S, 10.89. Beilstein test: Cl positive.^[50]

2.5. Procedure for the synthesis of compounds **5x–5y**

In a round bottom flask, 2,3-dichloro-1,4-naphthoquinone **1** (2.270 g, 10 mmol) and aryl amines **2a–b** (10 mmol) was mixed in double distilled water (700 mL). The reaction mixture was refluxed for 2 h. Once the reaction was complete, the mixture was cooled and the resulting precipitates were isolated, washed with hot water (500 mL), and dried at 45 °C. The crude product was then purified using column chromatography (silica gel column, 100–200 mesh) with a mixture of ethyl acetate and hexane (1:4 ratio). This process yielded compounds **5x–5y**.

2.5.1. 2-chloro-3-(phenylamino)naphthalene-1,4-dione (**5x**)

Deep maroon solid (96%); mp: 221–222 °C;^[51] IR (ATR): $\tilde{\nu}$ = 717, 1017, 1140, 1287, 1331, 1444, 1560, 1674, 3040, 3233. ^1H NMR (500 MHz, DMSO- d_6 , 25 °C, TMS): δ = 7.11–7.14 (m, 3H, Ar), 7.31 (t, J = 9.65 Hz, 2H, Ar), 7.79 (dt, J = 9.45 Hz & J = 1.30 Hz, 1H, Ar, quinone moiety), 7.86 (dt, J = 9.27 Hz & J = 1.40 Hz, 1H, Ar, quinone moiety), 8.02 (d, J = 9.50 Hz, 2H, Ar, quinone moiety), 9.29 (s, 1H, –NH) ppm. ^{13}C NMR (125 MHz, DMSO- d_6): δ = 114.2,

123.8, 124.2, 125.8, 126.2, 127.7, 130.0, 131.8, 132.9, 134.5, 138.6, 142.9, 176.4 (–C = O, quinone moiety), 179.8 (–C = O, quinone moiety) ppm. Anal. calcd for C₁₆H₁₀ClNO₂ (283): C, 67.74; H, 3.55; N, 4.94 Found: C, 67.69; H, 3.62; N, 4.91; Beilstein test: Cl positive.^[50]

2.5.2. 2-chloro-3-(*p*-tolylamino)naphthalene-1,4-dione (**5y**)

Light maroon solid (97%); mp: 204–205 °C; IR (ATR): $\tilde{\nu}$ = 718, 817, 1019, 1141, 1283, 1330, 1496, 1547, 1593, 1633, 1675, 2919, 3029, 3225. ¹H NMR (500 MHz, DMSO-*d*₆, 25 °C, TMS): δ = 2.29 (s, 3H), 7.02 (d, *J* = 10.2 Hz, 3H, Ar), 1.21 (q, *J* = 9.05 Hz, 2H, Ar), 2.51 (t, *J* = 8.90 Hz, 2H, Ar, quinone moiety), 2.29 (s, 3H, (–CH₃, *p*-tolyl moiety), 7.02 (d, *J* = 10.35 Hz, 2H, Ar, quinone moiety), 7.11 (d, *J* = 10.25 Hz, 2H, Ar, quinone moiety), 7.79 (dt, *J* = 9.25 Hz & *J* = 1.65 Hz, 1H, Ar, quinone moiety), 7.85 (dt, *J* = 9.27 Hz & *J* = 1.65 Hz, 1H, Ar, quinone moiety), 8.02 (dd, *J* = 9.37 Hz & *J* = 1.80 Hz, 2H, Ar, quinone moiety), 9.26 (s, 1H, –NH) ppm. ¹³C NMR (125 MHz, DMSO-*d*₆): δ = 20.6, 113.3, 124.1, 126.0, 126.5, 128.4, 130.2, 132.0, 133.1, 133.7, 134.8, 136.1, 143.2, 176.6 (–C = O, quinone moiety), 180.1 (–C = O, quinone moiety) ppm. Anal. calcd for C₁₇H₁₂ClNO₂ (297): C, 68.58; H, 4.06; N, 4.70. Found: C, 68.41; H, 3.98; N, 4.98; Beilstein test: Cl positive.^[50]

2.6. Procedure for the synthesis of compounds **5z–5aa**

Compounds **5x–5y** (4 mmol) were dissolved in acetonitrile (250 mL), followed by the slow addition of 1-propanethiol (0.371 g, 4 mmol). Subsequently, triethylamine (0.404 mL, 4 mmol) was introduced into the reaction mixture, which was then refluxed for 3 h. Upon completion of the reaction, the mixture was transferred to ice-cold water, resulting in the formation of a solid product that was filtered, dried at 45 °C, and purified using column chromatography (silica gel 100–200 mesh, ethyl acetate: hexane, 1:4) to yield compounds **5z–5aa**.

2.6.1. 2-(phenylamino)-3-(propylthio)naphthalene-1,4-dione (**5z**)

Deep maroon solid (99%); mp: 122–123 °C ^[52]; IR (ATR): $\tilde{\nu}$ = 753, 839, 913, 1015, 1085, 1128, 1183, 1282, 1440, 1495, 1588, 1660, 2869, 2954, 3059, 3284. ¹H NMR (500 MHz,

DMSO-*d*₆, 25 °C, TMS): δ = 0.76 (t, J = 9.10 Hz, 3H, –CH₃, propane thio moiety), 1.28 (q, J = 9.00 Hz, 2H, –CH₂, propane thio moiety), 2.52 (t, J = 8.20 Hz, 2H, –CH₂, propane thio moiety), 7.08 (d, J = 10.10 Hz, 3H, Ar), 7.30 (t, J = 9.95 Hz, 2H, Ar), 7.80 (dt, J = 8.90 Hz & J = 1.10 Hz, 1H, Ar, quinone moiety), 7.86 (dt, J = 8.75 Hz & J = 1.30 Hz, 1H, Ar, quinone moiety), 8.03 (t, J = 7.75 Hz, 2H, Ar, quinone moiety), 9.13 (s, 1H, –NH) ppm. ¹³C NMR (125 MHz, DMSO-*d*₆): δ = 13.0, 22.1, 34.7, 117.1, 122.1, 123.2, 125.9, 126.1, 127.8, 130.5, 132.9, 133.0, 134.4, 139.4, 145.6, 180.1 (–C = O, quinone moiety), 180.3 (–C = O, quinone moiety) ppm. Anal. calcd for C₁₉H₁₇NO₂S (323): C, 70.56; H, 5.30; N, 4.33; S, 9.91 Found: C, 70.40; H, 5.42; N, 4.31; S, 9.98.

2.6.2. 2-(propylthio)-3-(*p*-tolylamino)naphthalene-1,4-dione (**5aa**)

Deep maroon solid (99%); mp: 108–109 °C; IR (ATR): $\tilde{\nu}$ = 719, 818, 1015, 1134, 1284, 1495, 1562, 1589, 1636, 1688, 2919, 2960, 3339. ¹H NMR (500 MHz, DMSO-*d*₆, 25 °C, TMS): δ = 0.77 (t, J = 9.15 Hz, 3H, –CH₃, propane thio moiety), 1.30 (q, J = 9.05 Hz, 2H, –CH₂, propane thio moiety), 2.30 (s, 3H, –CH₃, Ar), 2.52 (t, J = 5.15 Hz, 2H, –CH₂, propane thio moiety), 6.99 (d, J = 10.30 Hz, 2H, Ar), 7.11 (d, J = 10.25 Hz, 2H, Ar), 7.79 (dt, J = 9.42 Hz & J = 1.10 Hz, 1H, Ar, quinone moiety), 7.85 (dt, J = 8.47 Hz & J = 1.45 Hz, 1H, Ar, quinone moiety), 8.02 (d, J = 9.60 Hz, 2H, Ar, quinone moiety), 9.00 (s, 1H, –NH) ppm. ¹³C NMR (125 MHz, DMSO-*d*₆): δ = 12.9, 20.4, 22.0, 34.7, 115.9, 122.3, 125.8, 126.0, 128.3, 130.5, 132.5, 132.8, 132.9, 134.4, 136.9, 146.1, 180.1 (–C = O, quinone moiety), 180.1 (–C = O, quinone moiety) ppm. Anal. calcd for C₂₀H₁₉NO₂S (337): C, 71.19; H, 5.68; N, 4.15; S, 9.50 Found: C, 71.10; H, 5.71; N, 4.42; S, 9.72.

2.7. Biology

2.7.1. Cell culture and in vitro cytotoxicity study

In this study, various human cancer cell lines were utilized, including A549 (lung carcinoma), SW480 (colorectal adenocarcinoma), MDA-MB-231 (triple negative breast carcinoma), and

MCF-7 (breast carcinoma) were obtained from the American type culture collection (ATCC, Manassas VA, 20110, United States) and Sigma-Aldrich (St. Louis, MO 63103, United States). Additionally, human normal cells, specifically HEK293 (human embryonic kidney cells), were also included in the investigation. All cells were incubated in DMEM or RPMI-1640 medium provided with fetal bovine serum (10%, Sigma-Aldrich Chemie GmbH, Steinheim, Germany), L-glutamine, and penicillin/streptomycin (Capricorn Scientific GmbH, Ebsdorfergrund, Germany) at an ambient temperature (37 °C, 5% CO₂). The effectiveness of the synthesized compounds (**3–5aa**, DMSO solvent) were checked with the cancer cells that were seeded in 96-well microculture plates at ten doses ranging from 0.195 μM, 0.390 μM, 0.781 μM, 1.56 μM, 3.125 μM, 6.25 μM, 12.5 μM, 25 μM, 50 μM, and 100 μM. After 24 h and 48 h treatment of cells with compounds, MTT solution (10 μL, 5 mg/mL in phosphate-buffered saline, PBS) was added. The formazan crystals were formed after 4 h incubation, that dissolved in DMSO (100 μL) and OD (optical density) was recorded at 590 nm. Triplicate tests were performed for all the compounds. All the IC₅₀ values were calculated using CalcuSyn software.^[53]

2.7.2. Morphological alterations study in MCF-7 cells

About 5×10^4 cells/well were seeded in a six-well plate and treated with 0 μM, 1.25 μM, 2.5 μM, 5.0 μM, and 10 μM of **5v** for 24 h and 48 h (37 °C, 5% CO₂). The cellular morphology was observed using an inverted microscope, images were captured with a use of ImageScope software (Aperio).^[54]

2.7.3. AO/EB double staining

Approximately 5×10^4 cells were plated in each well of a six-well plate and exposed to varying concentrations of **5v** (0 μ M, 1.25 μ M, 2.5 μ M, 5.0 μ M, and 10 μ M) for 24 h and 48 h (37 °C, 5% CO₂). Following treatment, the cells were fixed with 4% paraformaldehyde for 30 min at room temperature. Subsequently, the cells were stained with AO (10 μ g/mL) and EB (1 μ g/mL) before imaging under a fluorescent microscope.^[55]

2.7.4. Apoptosis study

MCF-7 cells were plated at a density of 1.2×10^6 cells per dish and exposed to varying concentrations of **5v** (0 μ M, 1.25 μ M, 2.5 μ M, 5.0 μ M, and 10 μ M) for 24 h. DMSO (0.01%) and doxorubicin (1.25 μ M, 2.5 μ M) were used as controls. Following treatment, the cells were detached using trypsin, centrifuged at 500 X g for 5 min at room temperature, washed with PBS, and subjected to flow cytometry analysis. Apoptosis induction in MCF-7 cells was assessed using the FITC Annexin V Apoptosis Detection Kit (BD Pharmingen) according to the manufacturer's instructions. Briefly, cells were harvested, washed with cold PBS, resuspended in 1X binding buffer (BD Pharmingen, kit component, 1×10^6 cells/mL), stained with FITC Annexin V/PI, and then analyzed using a flow cytometer (BD FACSCalibur flow cytometer, 1 Becton Drive Franklin Lakes, NJ, USA) after a 15 min incubation at room temperature in the dark.^[56]

2.7.5. Cell colony formation assay

MCF-7 single cell suspension was seeded in ϕ 100 mm cell culture dishes. Later, the cells were treated with a different concentration of **5v** (0 μ M, 1.25 μ M, 2.5 μ M, 5.0 μ M, and 10 μ M) for 24 h. After the treatment, the cells were harvested using TrypLE Express Enzyme (Gibco), counted using hemocytometer. The 200 and 350 cells of each variant were seeded in new cell culture dishes in duplicates. The cells were incubated and undisturbed for 10 days at 37 °C until cells in control dishes have formed sufficient clones consisting at least 50 cells.

Subsequently, the cells were fixed with 100% methanol for 20 min at room temperature and stained with 0.5% crystal violet in 25% methanol. The colonies were counted manually by light microscopy.^[57]

2.7.6. Data analysis

The surviving fraction (SF), representing the number of colonies that emerge after treatment, can be calculated using the following equation.

$$SF = \frac{\text{Number of colonies formed after treatment}}{\text{Number of cells seeded}} \times PE$$

Where, PE = plating efficiency.

2.7.7. Preparation of human cells extracts

MCF-7 cells were cultured in FBS-free DMEM. Then, the cells were treated with different concentration of **5v** (0 μ M, 1.25 μ M, 2.5 μ M, 5.0 μ M, and 10 μ M) for 24 h. After the treatment, the cells were harvested using TrypLE Express Enzyme (Gibco), centrifuged and according to protocol lysed (CellLytic™ MT Cell Lysis Reagent). Briefly, cells were incubated in ice with appropriate volume of lysis reagent on a shaker for 15 min. Subsequently, lysed cells were centrifuged for 10 min at 20000 X g to pellet the cellular debris. Finally, the supernatant portion was transferred to a chilled test tube.^[57]

2.7.8. SDS-PAGE and Western blotting

Exactly, 25 μ g total protein lysates were exposed to SDS-PAGE (10% polyacrylamide gel) under reducing conditions and it was transferred to polyvinylidene fluoride (PVDF, from Merck) membranes. The blots were preincubated in blocking buffer (1% nonfat dry milk in 10 mM TBS, pH = 7.4) for 1 h at room temperature. Then the protein lysates were further incubated with appropriate primary antibodies such as mouse anti-Bcl-2 monoclonal antibody (1/1000, v/v), mouse anti-Bax monoclonal antibody (1/1000, v/v), and mouse anti- α -tubulin monoclonal antibody (1/2000, v/v) in blocking buffer for 1 h. Next, the blots were washed with blocking buffer (contains 0.1% Tween 20) and incubated with alkaline phosphatase-conjugated

anti-mouse secondary antibodies (1/5000, v/v) for 1 h. The Bcl-2, Bax and tubulin protein bands were visualized using BCIP/NBT solution reagent after the treatment with different doses of compound **5v** (0 μ M, 1.25 μ M, 2.5 μ M, 5.0 μ M, and 10 μ M) for 24 h.^[58]

2.7.9. Cell cycle analysis

MCF-7 cells were incubated with **5v** (10 μ M) for 24 h. DMSO (0.01%) was used as a negative control. After the incubation, the cells were harvested by trypsinization, washed with PBS and pellets were fixed with ice-cold ethanol (1 mL, 80%) in -20 °C for 2 h. Lastly, the samples were subjected to flow cytometry analysis.^[59]

2.7.10. ROS detection

MCF-7 cells were seeded at 1.2×10^6 cell/dish and treated with **5v** (5 μ M) for 24 h. DMSO (0.01%) was used as a negative control. The pellets were suspended in CM-H₂DCFDA (1 mL, and 5 μ M) solution in PBS. For positive control, the untreated cells were washed three times with PBS and incubated with freshly prepared H₂O₂ (2 mM, 30 min at 37 °C) in PBS. After the incubation, the cells were harvested by trypsinization and incubated in the dark (37 °C for 30 min). Next, the cells were centrifuged at 130 X g for 5 min and gently resuspended in pre-warmed PBS. This step was repeated twice and the cells were submitted to flow cytometry ROS detection (excitation: 488 nm; emission: 535 nm). Parallely, 100 μ L cell suspension was stained with CM-H₂DCFDA (1 mL, 5 μ M), placed in a dark 96-well plate and fluorescence signal was measured using microplate reader (excitation: 488 nm; emission: 535 nm) in the end point mode.^[60]

2.8. *In vivo* analysis

2.8.1. Ecotoxicity

To assess the toxicity of **5v**, the fish embryo toxicity (FET) test was conducted on zebrafish larvae (*Danio rerio*) following the guidelines provided by the OECD Test Guideline 236. In this study, freshly fertilized zebrafish eggs were exposed to varying concentrations of **5v**,

ranging from 0 to 200 μM , for a duration of 96 h. The experimental setup employed a static system, ensuring that the changes in solution concentrations did not exceed 20% of the nominal concentration values.

The solution for xenograft model of MCF-7 cells (E3), which consisted of NaCl (5 mmol/L), KCl (0.17 mmol/L), CaCl_2 (0.33 mmol/L), MgSO_4 (0.33 mmol/L), with the pH of 7.2, served as both the embryo culture medium and the stock solution. The experiment took place in 24-well plates, with each well containing five embryos and a total of ten embryos per group. The plates were covered and placed in an incubator set at a temperature of 28 ± 0.5 °C, with a light/dark cycle of 12/12 h. Following the exposure period (96 hpf), the acute toxicity was evaluated by monitoring four visual indicators of lethality. These indicators included the formation of clots in fertilized eggs, the absence of somite development, the failure of the tailbud to detach from the yolk sac, and the lack of a heartbeat. The LC_{50} value was calculated to determine the toxicity level. Furthermore, the heart rate was measured to determine the potential cardiotoxic effects of **5v**.^[61] A statistical analysis utilizing one-way ANOVA was conducted employing GraphPad 9 software (version 9.0.0 for Windows, GraphPad Software, Boston, Massachusetts, USA, www.graphpad.com).

2.8.2. *Xenotransplantation of MCF-7 cells*

2.8.2.1. *Cell labelling and Zebrafish xenografts*

MCF-7 cells were suspended at a density of $1 \times 10^6/\text{mL}$ were labelled (Vybrant™ DiI Cell-Labeling Solution, Thermo Fisher Scientific, Waltham, MA, USA) at a concentration of 5 $\mu\text{L}/\text{mL}$ according to manufacturer's instructions. 2 dpf zebrafish embryos were anaesthetized with tricaine (0.003%, Sigma-Aldrich, St. Louis, MO, USA) and placed on a Petri dish (10 cm) that coated with 1% agarose. The labelled MCF-7 cell suspension was introduced into the yolk sac by microinjection in the amount of 2 nL (~300 cells/embryo). The suitable injected embryos were selected after 2 hpi (hours post injection).^[62]

2.8.3. Zebrafish xenograft drug administration

The selected embryos were randomly divided into 3 groups: two groups of larvae were treated with **5v** at two different doses: 2 μM , and 10 μM , while one another group of larvae was not treated. All larvae were placed at 31 °C for 72 h. As per Directive 2010/63/EU, which focuses on safeguarding animals utilized for scientific purposes, zebrafish are classified as self-feeding larval forms until 120 hpf, *i.e.*, initial 5 days of their life. Therefore, zebrafish are not regarded as animals and do not necessitate ethical approval from authorities.^[50] At the end of observation period, the images of the fish from each group were taken to monitor the growth of tumour cells (Discovery V8 Stereo optical microscope and Zeiss hardware).^[63]

2.9. *In silico* analysis

To understand the interaction between the synthesized compound **5v** and cancer cell proteins, an *in silico* molecular docking study was carried out with the receptors such as the estrogen receptor (ER), epidermal growth factor receptor kinase (EGFR), breast cancer type 1 susceptibility protein (BRCA1), and vascular endothelial growth factor receptor 2 (VEGFR2) were obtained from the PDB databank under accession numbers 3ERD, 6S9C, 4Y2G, and 2XIR, respectively. Compound **5v** and the standard anticancer drug doxorubicin was selected as final targets for the molecular docking study. Molecular docking was conducted utilizing AutoDock Vina software.^[64] A grid box was strategically selected to encompass the entire receptor, facilitating global docking analysis. The outcomes of the global docking led to the identification of a local binding site that corresponded with the co-crystallized ligand. The grid spacing was established at 0.375 Å, and the grid box was centered on the receptor's active site, measuring 20 Å × 20 Å × 25 Å to guarantee comprehensive coverage of the binding site. Three separate docking runs were executed, each comprising 100 search iterations. Additionally, the docking results were validated through cross-docking with doxorubicin at the binding site indicated in the PDB entry or within the co-crystallized structure. The RMSD values of **5v** in

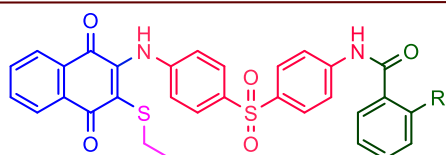
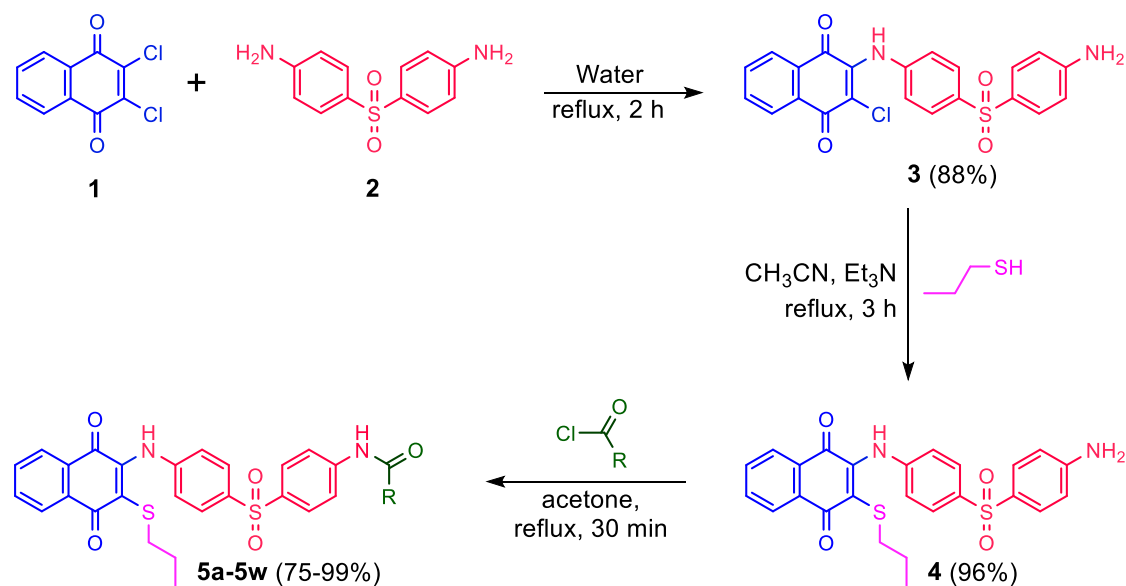
relation to doxorubicin at the binding site were determined by superimposing the two docked complexes utilizing the PyMOL software package. A lower RMSD value, along with a higher docking score, suggests a potentially more robust or advantageous binding interaction with the receptor. 3D structure of doxorubicin was obtained from PubChem (PubChem CID:31703). The compound **5v** and doxorubicin were optimized at the Becke, 3-parameter, Lee–Yang–Parr (B3LYP) level of theory, and the 6-31G* basis set using the Gaussian 09 software package. Docking score (kcal/mol) was used to determine the docking output of the molecules.^[65] Furthermore, the theoretical Absorption, Distribution, Metabolism and Excretion (ADMET) profiles of **5v** was calculated using the molinspiration tool. The pharmacokinetics of **5v** were obtained using admetSAR and swissADME.^[66] All the chemical structures were drawn using ACD/chemsketch.

3. Results and discussion

3.1. Chemistry

A novel library of 1,4-naphthoquinone containing 1-propanethio moiety were synthesized (Schemes 1 and 2). As per our previous report, the parental compound **3** was synthesized from 2,3-dichloro-1,4-naphthoquinone **1** and dapsone **2** through the nucleophilic substitution reaction.^[49] Next, the compound **4** was synthesized *via* nucleophilic substitution of compound **3** and 1-propanethiol in dry acetonitrile. An equimolar amount of base triethylamine was used to catalyze the reaction for 3 h and the compound **4** was obtained with a 96% yield. The same reaction was performed in various organic and aqueous solvents including water, acetone, ethanol, methanol, dimethyl sulfoxide, and dimethylformamide; though, several byproducts were alongside with the compound **4**. Finally, compound **4** was used to synthesize the expected compounds **5a–w**. Compound **4** was benzoylated or acylated with several acid chlorides in acetone with 30 min reflux that afforded the desired compounds in good yield (75–99%; Scheme 1). Also, compounds **5x–5aa** were synthesized using our previously reported method

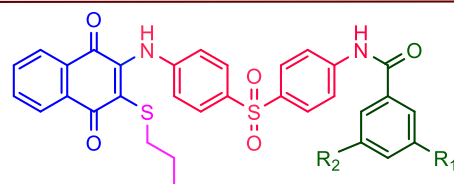
with minor modifications.^{[67],[46]} The desired products were isolated in a moderate to good percentage yield (96–99%; Scheme 2).



5a R = H (86%)

5b R = F (92%)

5c R = Br (88%)

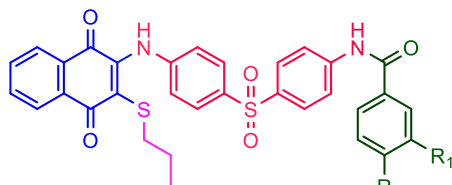


5d R¹ = CF₃, R² = H (75%)

5e R¹ = Cl, R² = Cl (84%)

5f R¹ = NO₂, R² = NO₂ (98%)

5g R¹ = NO₂, R² = H (99%)



5h R¹ = NO₂, R² = OCH₃ (99%)

5i R¹ = NO₂, R² = Cl (95%)

5j R¹ = H, R² = OCH₃ (87%)

5k R¹ = H, R² = CH₃ (84%)

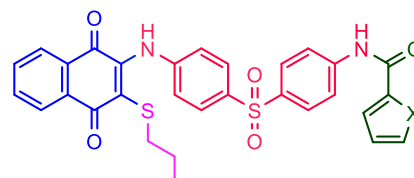
5l R¹ = H, R² = *t*-Bu (98%)

5m R¹ = H, R² = F (94%)

5n R¹ = H, R² = Cl (99%)

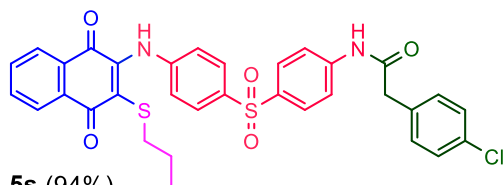
5o R¹ = H, R² = Br (95%)

5p R¹ = H, R² = NO₂ (85%)

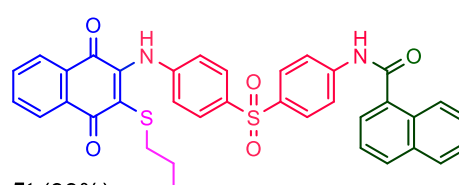


5q X = O (96%)

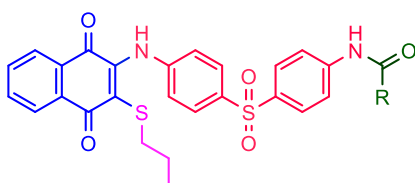
5r X = S (98%)



5s (94%)



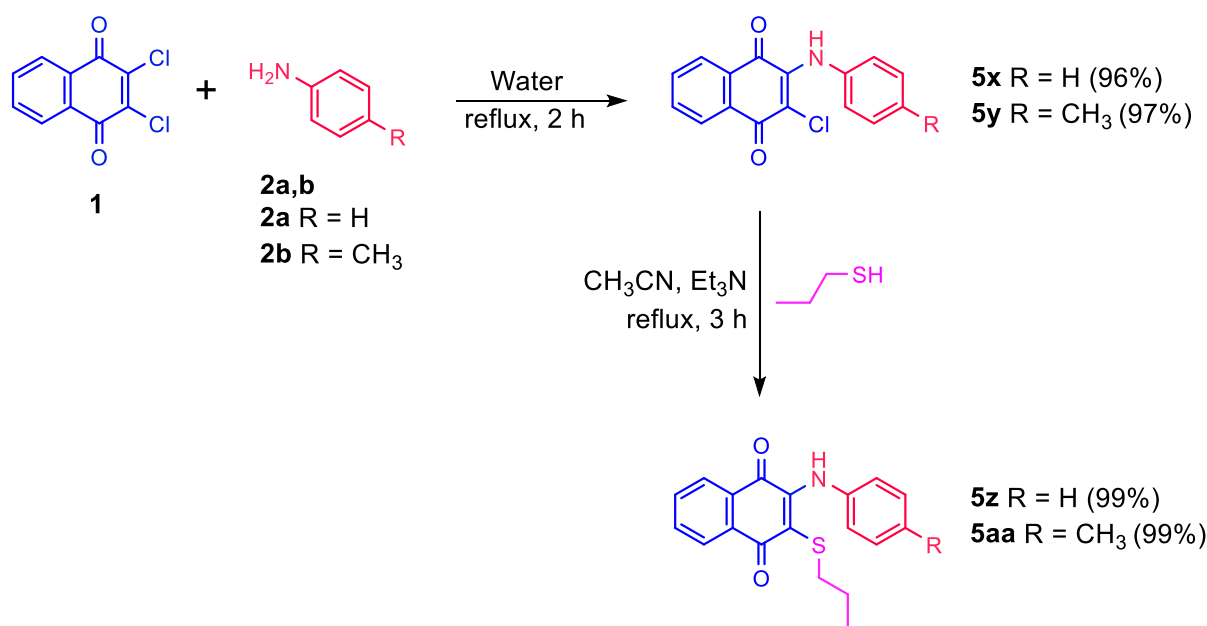
5t (99%)



5u R = Et (88%)

5v R = CH₃ (75%)

5w R = CH(Cl)₂ (93%)

Scheme 1. Synthesis of diversly substituted 1,4-naphthoquinone derivatives (**3–5w**).**Scheme 2.** Synthesis of aryl amino naphthoquinones (**5x–5aa**).**3.2. In vitro biological studies****3.2.1. Cytotoxicity study**

All the synthesized naphthoquinones **3–5aa**, were studied for their cytotoxic property by MTT assay^{[68],[69]} using four human cancer cell lines including A549 (lung carcinoma), SW480 (colorectal adenocarcinoma), MDA-MB-231 (triple negative breast carcinoma), MCF-7 (breast carcinoma) and human normal cells including HEK293 (human embryonic kidney cells). The selection of human cancer cell lines was based on their ability to represent the most prevalent types of cancers globally, considering both their incidence and mortality rates.^{[70],[71]} The anticancer drug doxorubicin (DOX) was utilized as a standard drug. The cytotoxicity study of all the compounds (**3–5aa**) was carried out at two different incubation period such as 24 h and 48 h. Cytotoxicity was defined as the concentration needed to cause a 50% loss of the cell monolayer (IC₅₀, Table S1).

Amongst, compounds **5i**, **5l**, **5o**, **5q**, **5r**, **5s**, **5t**, and **5v** showed significant cytotoxic property which is higher than the standard drug doxorubicin. Specifically, compound **5v** showed superior cytotoxicity against all the tested cancer cell lines. Compounds **5r** ($IC_{50} = 1.2 \mu\text{M}$, and $1.1 \mu\text{M}$ at 24 h and 48 h, respectively) showed potent cytotoxic activity against A549 cells with comparable IC_{50} values to that of doxorubicin ($IC_{50} = 2.3 \mu\text{M}$, and $2.1 \mu\text{M}$ at 24 h and 48 h, respectively). Compounds **5q** ($IC_{50} = 4.9 \mu\text{M}$, and $1.2 \mu\text{M}$ at 24 h and 48 h, respectively) showed potent cytotoxic activity against SW480 cells with comparable IC_{50} values to that of doxorubicin ($IC_{50} = 6.9 \mu\text{M}$, and $5.1 \mu\text{M}$ at 24 h and 48 h, respectively). Compounds **5v** ($IC_{50} = 1.5 \mu\text{M}$, and $1.3 \mu\text{M}$ at 24 h and, 48 h, respectively) showed potent cytotoxic activity against MDA-MB-231 cells with comparable IC_{50} values to that of doxorubicin ($IC_{50} = 10.6 \mu\text{M}$, and $9.1 \mu\text{M}$ at 24 h and, 48 h, respectively). With respect to MCF-7 breast carcinoma, compound **5v** ($IC_{50} = 1.2 \mu\text{M}$, and $0.9 \mu\text{M}$, at 24 h and, 48 h, respectively) was the highly active cytotoxic agent and showed potent activity than doxorubicin ($IC_{50} = 2.4 \mu\text{M}$, and $2.1 \mu\text{M}$ at 24 h and, 48 h, respectively). The compounds (**3–5aa**) exhibited higher IC_{50} values against HEK293 cells, indicating the non-toxic nature of the compounds in normal human cells. Additionally, the cytotoxicity assay was conducted for all the compounds at two different incubation times: 24 h and 48 h. The cytotoxicity of the compounds (**3–5aa**) was found to be slightly more effective after 48 h of treatment compared to 24 h. The extended cytotoxic investigation shows that the compounds remain stable and retain their cytotoxic effect even after 48 hours.

To verify the selectivity index (SI) and safety profile of the synthesized naphthoquinones (**3–5aa**), the toxicity study was carried out in normal HEK293 cell line (human embryonic kidney cells). The SI values are calculated from the IC_{50} of HEK293 cell line (non-cancer cells) divided by MCF-7 cell line (cancer cells) and are listed in Table S1. All the studied compounds exhibited less toxicity against HEK293 cell line, in comparison with

the standard drug doxorubicin ($IC_{50} = 9.5 \mu\text{M}$, and $12.3 \mu\text{M}$ at 24 h and 48 h, respectively). The calculated SI values of all the compounds (**3–5aa**) are higher than 2 (2.00 – 47.00) which indicate that the compounds are more selective towards the human cancer cells and less toxic towards the human normal cells.^[72]

The obtained results prompted an investigation into the SARs (structure-activity relationships) of the synthesized compounds (**3–5aa**). Incorporating a thio moiety at the C–3 position of the naphthoquinone ring resulted in enhanced cytotoxicity than the parent compound **3**. Notably, forming amides of compound **4** with different acid chlorides that significantly enhanced the inhibitory activity. The compounds (**3–5aa**) demonstrated significant cytotoxicity against all four cell lines, specifically, with aryl amides containing electron-donating or electronegative functional groups exhibiting superior efficacy compared to doxorubicin (**5i**, **5l**, **5o**, **5s**, and **5t**). It is important to highlight that the amide linkage with the extended heterocyclic moiety (**5q** and **5r**) showed a strong cytotoxic effect against the cell lines. Conversely, compounds with electron-withdrawing functional groups displayed lower inhibitory activity (**5f** and **5g**). It is important to highlight that the compounds in Schemes 1 & 2, specifically the aryl amino-sulfanyl, thio, and amide counterparts, play a crucial role in improving the cytotoxic properties. Out of all the compounds examined for their cytotoxic effects on four different human cancer cell lines (A549, SW480, MDA-MB-231, and MCF-7), **5v** exhibited the strongest cytotoxic activity. Interestingly, **5v** demonstrated significant activity against the MCF-7 cell line, displaying high SI values and a favourable safety profile. Consequently, additional *in vitro* and *in vivo* investigations were carried out to explore the mechanism of action of **5v** in cancer cell

3.2.2. Morphological alterations study in MCF-7 cells

The cancer cell growth and apoptotic properties can be observed through the significant morphological changes. Following drug treatment, the cells undergo apoptosis and their shape transforms into a round shape. To examine the impact of **5v** on the structure of MCF-7 cells, different time intervals of 24 h and 48 h were considered in a dose-dependent manner (Fig. 3a & b). MCF-7 human cancer cells were exposed to varying concentrations of **5v**, while DMSO served as the negative control. After the treatment of **5v** with MCF-7, significant morphological changes were found in cells treated with 1.25 μM , 2.5 μM , 5.0 μM and 10 μM of **5v** as compared to untreated control cell population. Treated cells lost their typical morphologic features and adhesion properties such as adherence to the surface, and cell to cell attachment. Detached cells had a tendency to form clusters of small number of cells floating in the medium. Shrinkage of the cells was highly noticeable and decrease of cell number was also observed when compared to the control (white cells). After 48 h cell treatment that exhibited even higher sensitivity to the compound **5v** which characterized by membrane blebbing and forming apoptotic bodies. Consequently, the findings suggest that the treatment of **5v** had an impact on cell death in MCF-7 cells, leading to apoptosis following exposure to different concentrations of **5v**. Besides, the results highlight the importance of **5v** in triggering apoptosis in MCF-7 cells. Furthermore, the observations suggest that **5v** exhibits higher cytotoxicity in MCF-7 cells, as evidenced by alterations in cancer cell morphology.

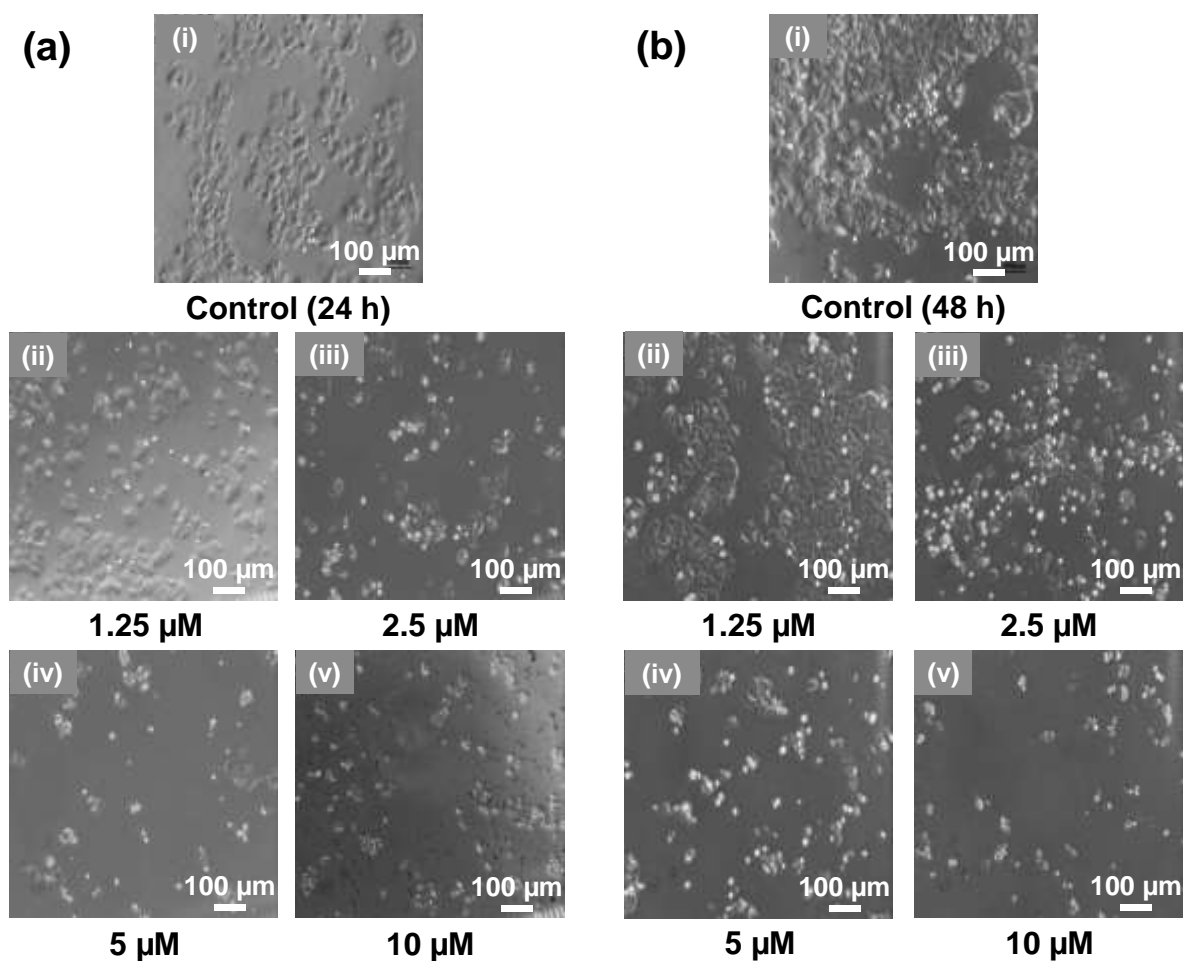


Fig. 3. The compound **5v** causes the cell death in MCF-7 cells; (a) Treated MCF-7 cells with DMSO and different concentration of **5v** for 24 h; (b) Treated MCF-7 cells with DMSO and different concentration of **5v** for 48 h. The cellular morphology was documented using bright field imaging.

3.2.3. AO/EB double staining assay

AO/EB double staining assay was used to evaluate the effect of compound **5v** in MCF-7 cell line for 24 h and 48 h. As shown in Fig. 4, AO/EB staining cells were observed using fluorescent microscope in order to discriminate the live, apoptotic and necrotic cells. The results showed various changes in the morphology and shape of the cells. The untreated cells exhibit green fluorescence. The cells treated with 1.25 μM concentration of **5v** do not show any significant changes in fluorescence. Early apoptotic cells exhibiting yellowish/orange fluorescence appeared after 2.50 μM treatment. With the increased concentration of **5v** (5.0

μM and $10.0 \mu\text{M}$), the number of early apoptotic cells increased, while at the same time, cell adherence was decreased and loss of the capacity to form dense colonies are noticeable. Especially, with the treatment of $10 \mu\text{M}$ of **5v**, the ratio of yellow/orange and orange/red to green fluorescent cells were appeared in higher amount. These results indicate that the compound **5v** showed the anticancer activity *via* apoptosis and necrosis pathways.

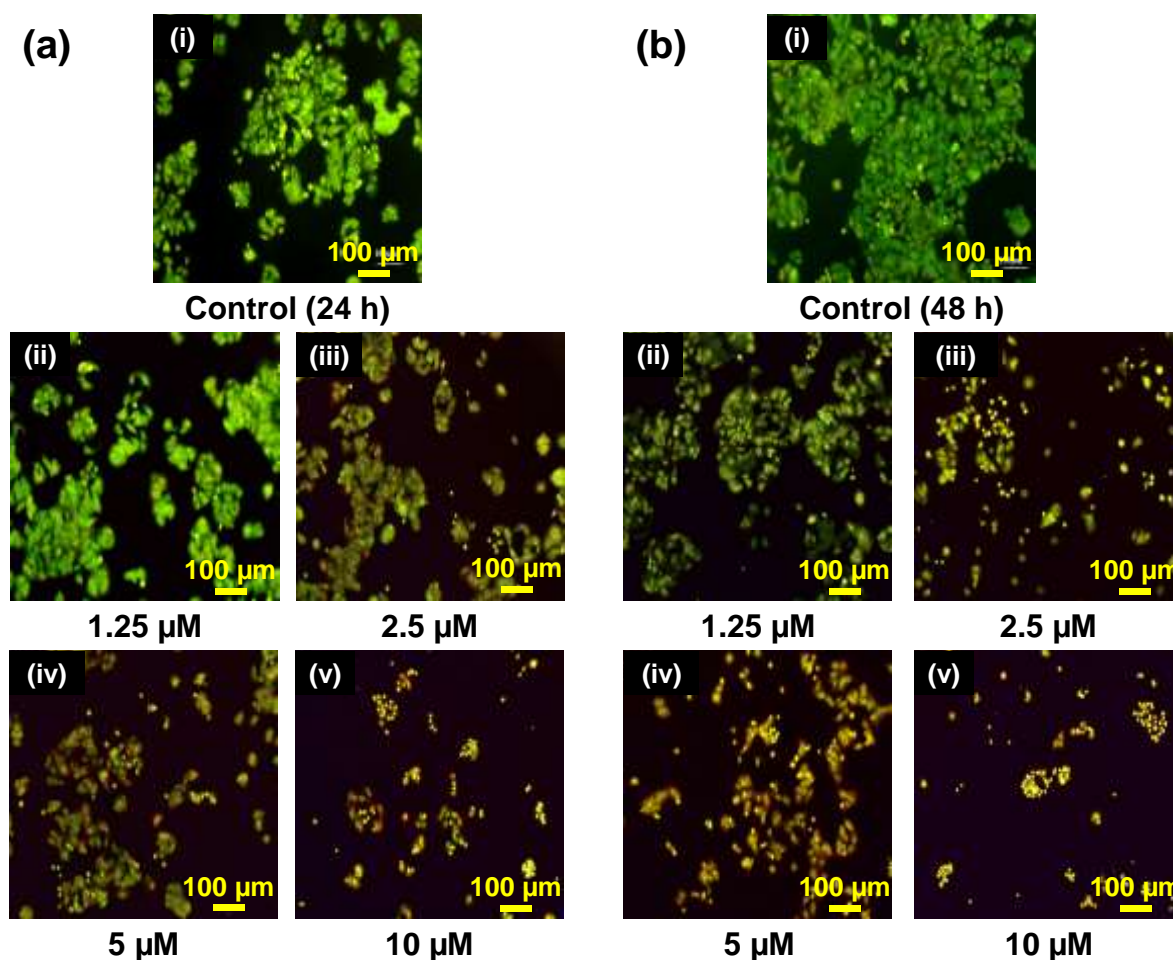


Fig. 4. (a) Detection of apoptosis by AO/EB staining in MCF-7 cell line after 24 h treatment; (b) Detection of apoptosis by AO/EB staining in MCF-7 cell line after 48 h treatment. Where, green coloured cells = live cells; yellow/orange-coloured cells = early apoptotic cells; orange/red-coloured cells = late apoptotic cells; red-coloured cells = necrotic cells.

3.2.4. Apoptosis study

To investigate the cell apoptosis induced by the compound **5v** in MCF-7, the apoptosis assay was performed using the Annexin V-FITC/propidium iodide double staining method. The

effect of **5v** on the induction of apoptosis in MCF-7 cells is showed in Fig. 5 & Table 2. These results showed the enhancement of the total apoptotic and necrotic cells percentage after the treatment of **5v** in MCF-7 cell on dose-dependent manner. For **5v** with 1.25 μM , higher apoptotic cells (5.05%), and necrotic cells (20.99%) were observed in comparison to the control cells (8.20%, and 11.79%), and doxorubicin (0.67%, and 16.44%, respectively). Meanwhile, with the increasing concentration of **5v** up to 10 μM , **5v** showed an increase of the total necrotic cell percentage in MCF-7 cells (65.29%) relative to the control cells (11.79%). Furthermore, **5v** showed better apoptotic and necrotic cells death in contrast to the standard doxorubicin. These results suggested that the compound **5v** could be the potent apoptotic and necrotic inducer.

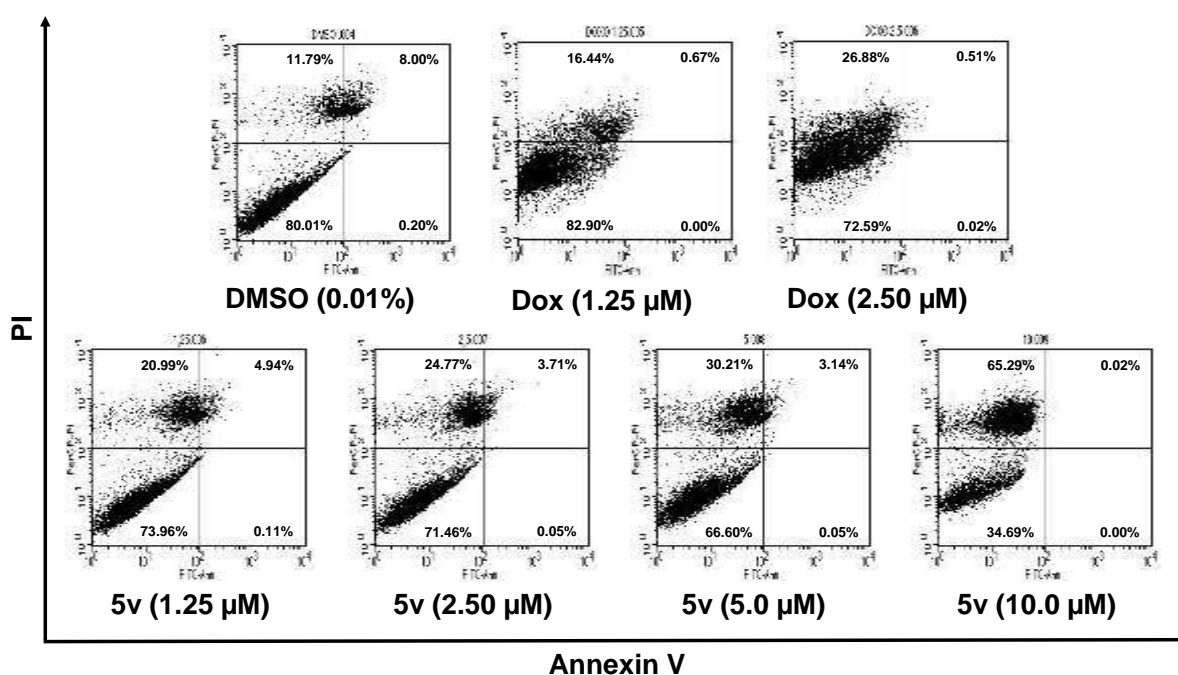


Fig. 5. Apoptotic and necrotic study was performed in MCF-7 cells by Annexin V-FITC/PI double staining assay. All the experiments were performed in triplicates.

Table 2. Apoptotic effect of compound **5v** in MCF-7 cells.

| Compound | Apoptosis % | | | Necrosis % | Total % \pm SD |
|----------|-------------|--------|---------|------------|------------------|
| | Early % | Late % | Total % | | |
| Control | 0.20 | 8.0 | 8.20 | 11.79 | 19.99 \pm 0.59 |

| | | | | | |
|--------------------------|------|------|------|-------|------------------|
| Dox (1.25 μ M) | 0.0 | 0.67 | 0.67 | 16.44 | 17.11 \pm 1.23 |
| Dox (2.50 μ M) | 0.02 | 0.51 | 0.53 | 26.88 | 27.41 \pm 0.92 |
| 5v (1.25 μ M) | 0.11 | 4.94 | 5.05 | 20.99 | 26.04 \pm 0.15 |
| 5v (2.50 μ M) | 0.05 | 3.71 | 3.76 | 24.77 | 28.53 \pm 0.68 |
| 5v (5.0 μ M) | 0.05 | 3.14 | 3.19 | 30.21 | 33.40 \pm 0.26 |
| 5v (10.0 μ M) | 0.0 | 0.02 | 0.02 | 65.29 | 65.49 \pm 0.51 |

*Dox-Doxorubicin

3.2.5. Cell colony formation assay

Along with MTT assay, the anticancer effect of lead compound **5v** was evaluated in a dose-dependent manner using the cell colony formation assay. The results indicate that the survival fraction of the MCF-7 cells after **5v** (2.50 μ M, and 5.0 μ M) treatment was reduced to about 52% and 75% in comparison to the control cells, respectively. Interestingly, at applying 10 μ M of **5v**, the MCF-7 cell line growth was completely arrested after 24 h of drug exposure. The cell colony formation activity was compared with the standard drug doxorubicin (5 μ M) which showed 2.12-fold lesser inhibition activity than the compound **5v** (Fig. 6).

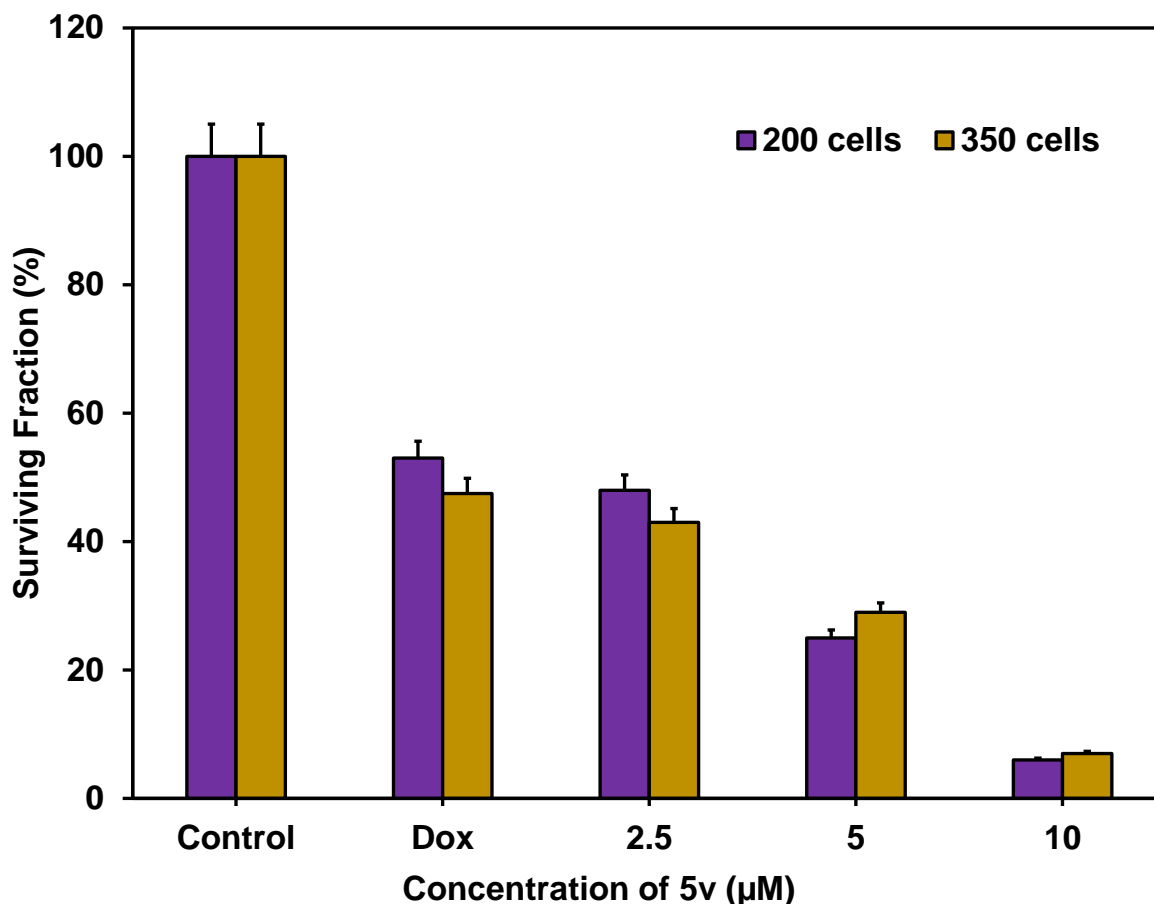


Fig. 6. Cell colony formation assay of at various concentrations of **5v** against MCF-7 cell line. All the experiments were performed in triplicates.

3.2.6. SDS-PAGE and Western blotting

The gene and protein expression of Bax (proapoptotic), and Bcl2 (antiapoptotic) in MCF-7 cells exposed to **5v** were analyzed (Fig. 7). The obtained results indicate that MCF-7 cell expression pattern of Bax was higher than doxorubicin. Alongside, Bcl-2 expression in MCF-7 cells was reduced significantly after 24 h, signifying that this was the source of mitochondrial permeability (Fig. 7a–e).^[73] Besides, the results validate that a high ratio of Bax to Bcl-2 can result in the release of tubulin, so activating apoptosis (Fig. 7f–g).^[74] The obtained results support the aforementioned statement that there was a gradual increase in the gene and protein expression patterns of tubulin. Furthermore, it has been demonstrated that tubulin is released from mitochondria during the initial phases of apoptosis.^[2] Our research findings suggest that

the initiation of apoptotic cell death in MCF-7 is a two-step process involving the release of tubulin from mitochondria, which subsequently triggers the activation of Bax and Bcl-2.

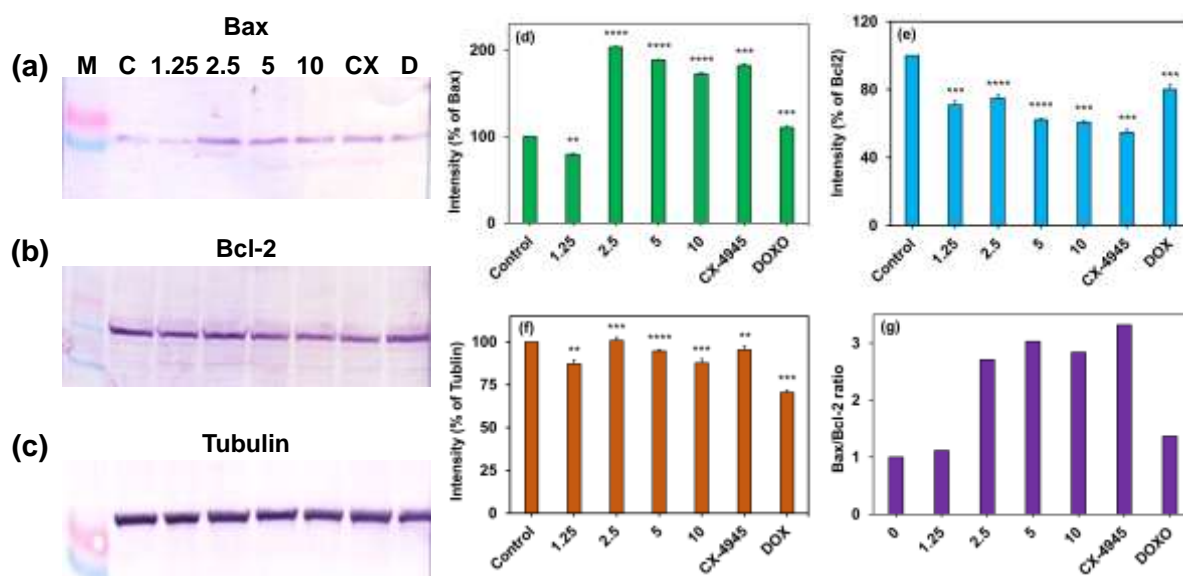


Fig. 7. (a–c) The molecular pathways of MCF-7 cells treated with varying concentrations of **5v** (1.25 μ M–10 μ M) involve both pro- and antiapoptotic genes; (d–f) The gene expression pattern in these cells was analyzed using semiquantitative RT-PCR for different genes; (g) The quantification of mRNA expression revealed fold level changes in MCF-7 cells. Statistical significance was determined based on *p*-values, with values <0.0001 (****), 0.0001 (***), 0.0025 (**), and ns (non-significant) considered significant. Standards: doxorubicin (20 μ M) and CX-4945 (20 μ M). All the experiments were performed in triplicates.

3.2.7. Cell cycle analysis

Compound **5v** underwent testing to determine its impact on cell cycle arrest in the MCF-7 cell line. The flow cytometry results (Fig. 8) showed that **5v** significantly increased the DNA percentage content isolated in S phase by elevating cellular population from 11.33% to 36.48% against MCF-7 cell line. These results indicate that the mechanism of anti-breast cancer mode of **5v** was induced by cell cycle arrest at S phase.

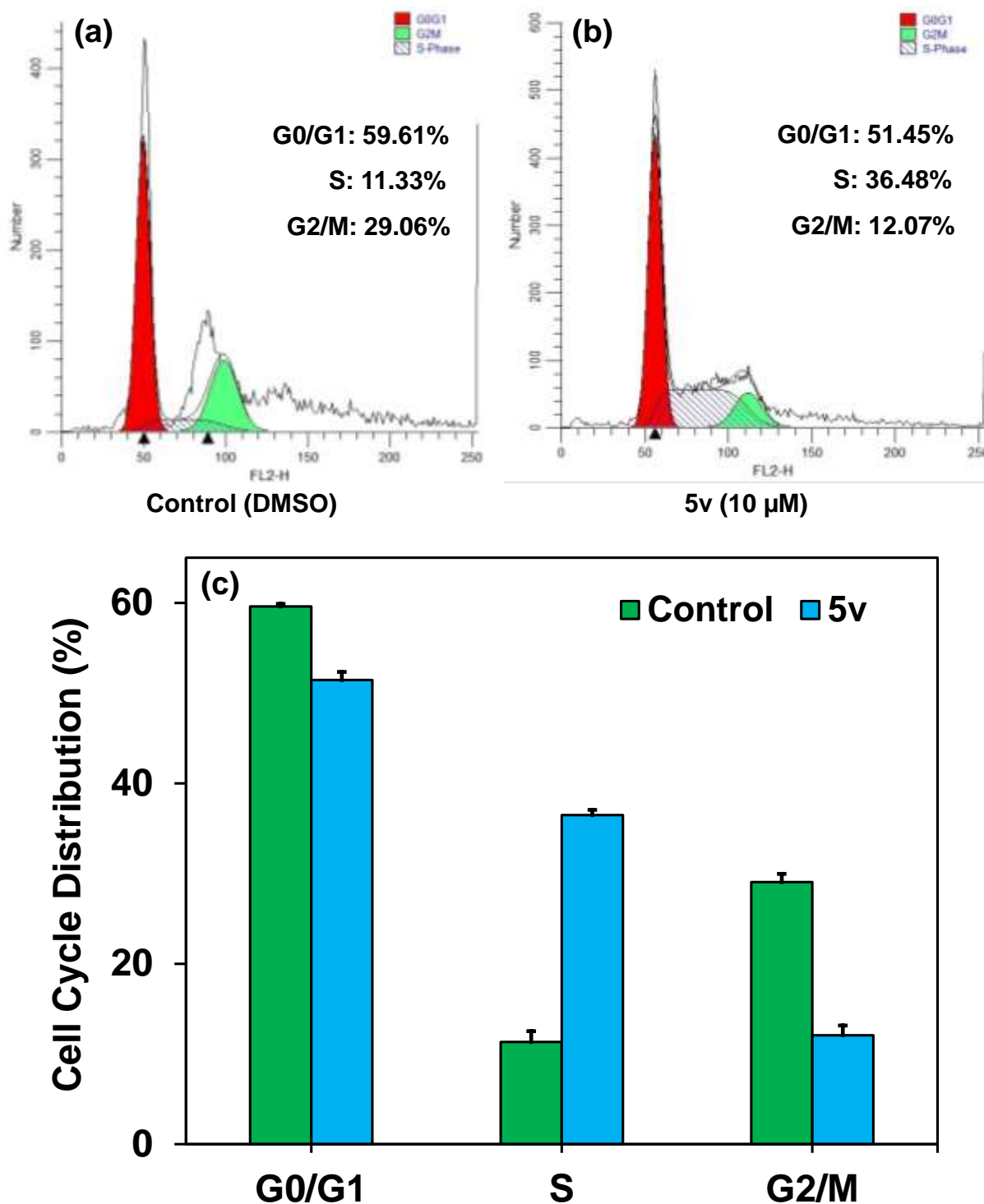


Fig. 8. (a, b) Effect of **5v** on the cell cycle of MCF-7 cell line after 24 h compared to control; (c) Statistical analysis of cell cycle in MCF-7 cells treated with **5v**. All the experiments were performed in triplicates.

3.2.8. ROS detection

Compound **5v** was found to make cell death by producing damage to proteins, lipids, DNA, and RNA through increased levels of reactive oxygen species (ROS). To assess the ROS production induced by **5v**, DCFH-DA dye was utilized. DCFH-DA is a commonly used fluorescent dye for ROS detection in cells. The oxidation of DCFH by ROS results in the production of DCF, emitting green fluorescence that can be visualized using a fluorescence microscope.^[75] A dose-dependent increase in ROS production was observed in MCF-7 cells treated with **5v** (Fig. 9). The generation of ROS was 3.7, and 1.05-fold higher for **5v** compared to the negative (DMSO) and positive (H_2O_2) control cells, respectively. These findings suggest that **5v** is responsible for ROS production, which may be one of the mechanisms leading to MCF-7 cell death.

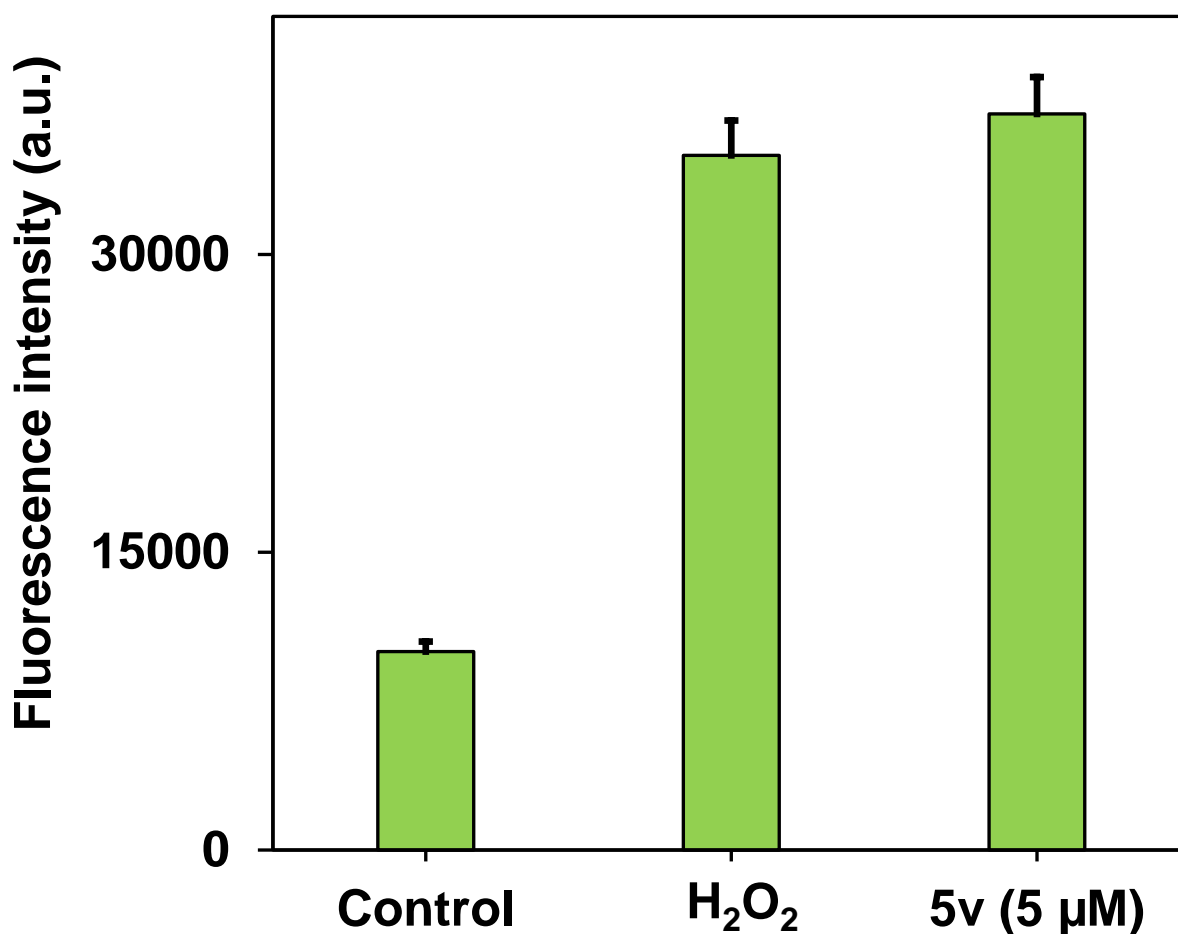


Fig. 9. ROS generation study of **5v** in MCF-7 cell line. All the experiments were performed in triplicates.

3.3. *In vivo* analysis

3.3.1. *Ecotoxicity*

Zebrafish model is a perfect animal model being able to evaluate the anticancer efficiency of small organic molecules. The current study focused on examining the ecotoxicity of compound **5v** using the *Danio rerio* animal model. Treatment of **5v** at the various concentrations (0, 2.5, 5.0, 7.5, 10.0, 15.0, 25.0, 50.0, 75.0, 100.0, 150.0, and 200.0 μM) for 96 hpf (hours post fertilization), the ecotoxicity profile was evaluated. All investigated concentrations were found nontoxic (Fig. 10a). Furthermore, to determine the potential impact on the cardiotoxicity, the heart rate was measured. Interestingly, the results indicate that the compound **5v** displayed insignificant impact on cardiac functions (Fig. 10b). Though, at higher dosage (50 μM), edema were observed at pericardial, yolk, and stripe areas (Fig. 10c). Thus, the ecotoxicological investigation of **5v** in zebrafish larvae specifies that the compound **5v** is harmless to use in living systems. From the obtained investigations, the LC_{50} (lethal concentration) value of **5v** was determined as 50.15 μM (the dose that causes mortality of 50% of fish) that indicate that the compound **5v** is non-toxic to the animal model.

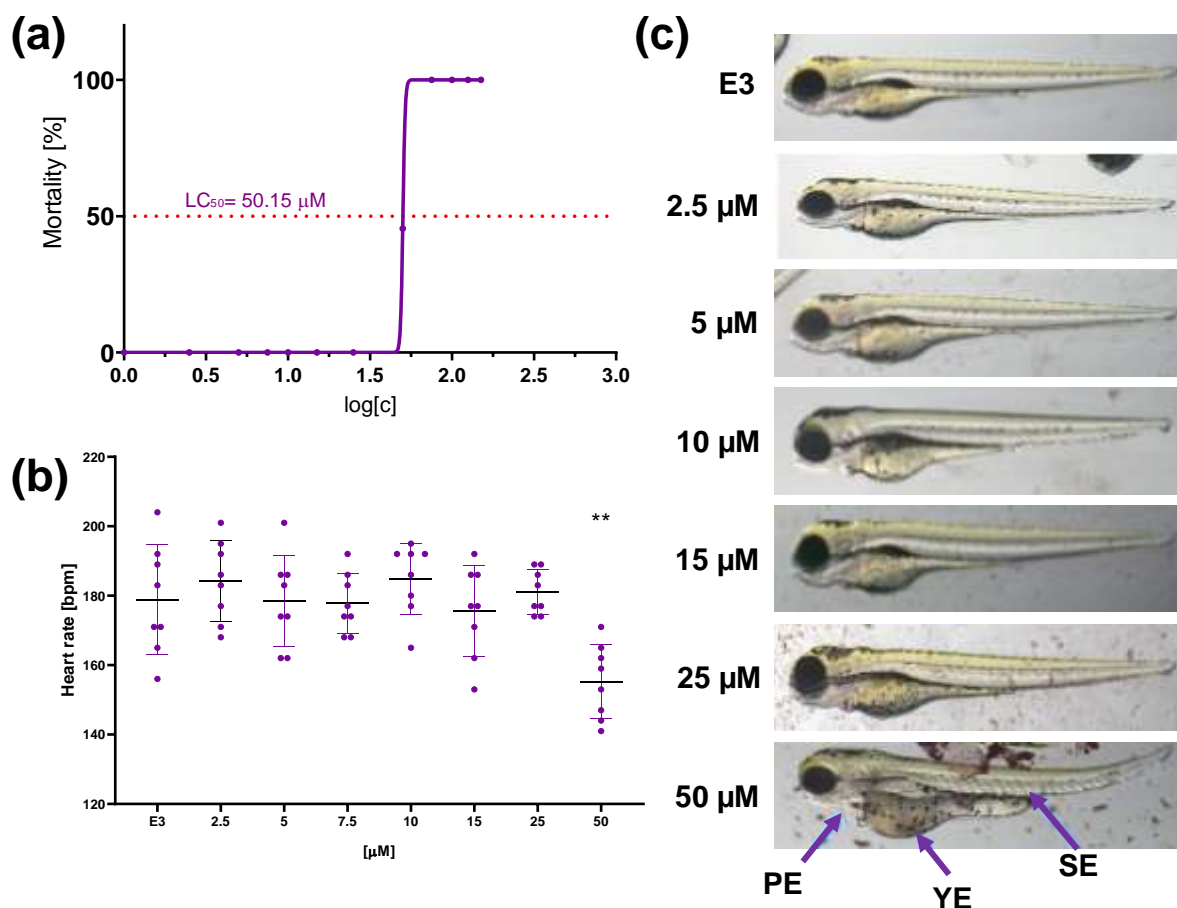


Fig. 10. The ecotoxicological investigation of **5v**; (a) toxicological profile of **5v** in zebrafish larvae; (b) cardiological functions of **5v** in zebrafish larvae. Where PE = pericardial edema; YE = Yolk edema; and SE = Stripe edema. The experiments were performed in uniplicate. ANOVA post hoc Tukey test: * $p < 0.05$, ** $p < 0.01$, *** $p < 0.001$.

3.3.2. Xenotransplantation of MCF-7 cells in zebrafish larvae

Zebrafish xenograft studies provide the information to visualize various aspects of tumor death cycle.^[76] To evaluate the anticancer potential of **5v** at various concentrations, we implanted MCF-7 cells into 2 dpf (days post fertilization) zebrafish larvae (Fig. 11a,b). Three days after implantation, the fluorescence intensity of the the MCF-7 cells were measured and it had almost disappeared from the xenograft, whereas about 95% of **5v** xenografted zebrafish larvae survived after 10 days of the treatment. Moreover, normal growth was observed without the existence of the implanted MCF-7 cells. Together, the ecotoxicity and xenotransplantation of

MCF-7 cells in zebrafish larvae studies indicate that the compound **5v** more specific and active towards the breast cancer cells such as MCF-7. The results implies that **5v** act as an anticancer agent through the mitochondria-mediated apoptotic signaling pathway (Fig. 12).

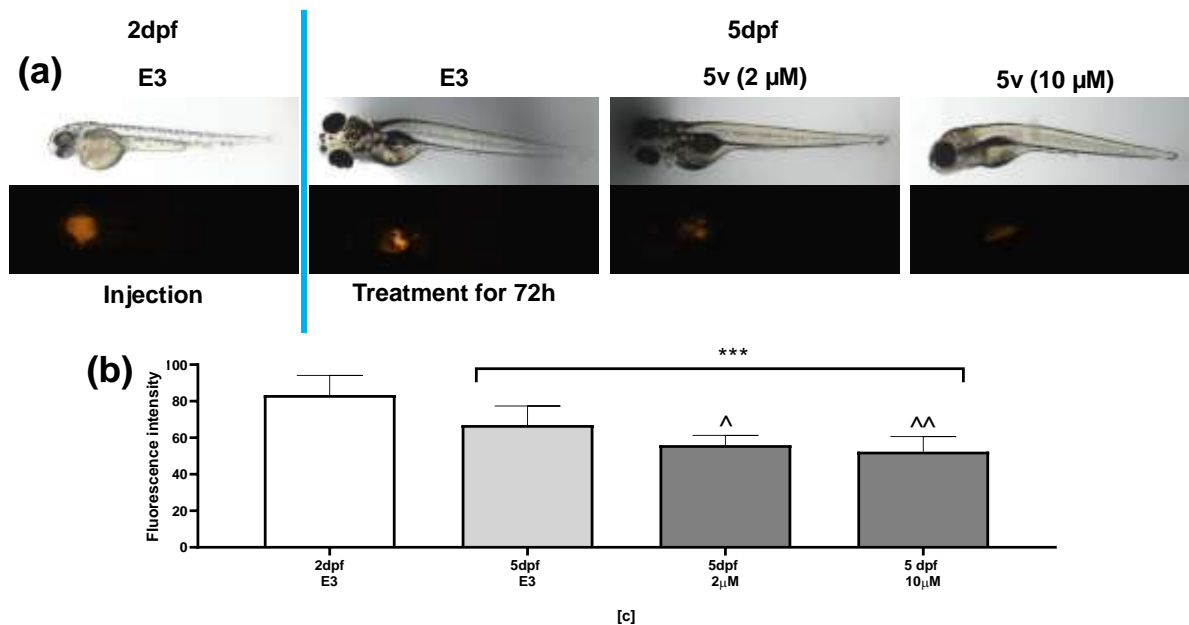


Fig. 11. (a) The xenotransplantation study of **5v** in zebrafish larvae; (b) fluorescence intensity of MCF-7 cells in the zebrafish larvae; where E3 = xenograft model of MCF-7 cells. All the experiments were performed in triplicates.

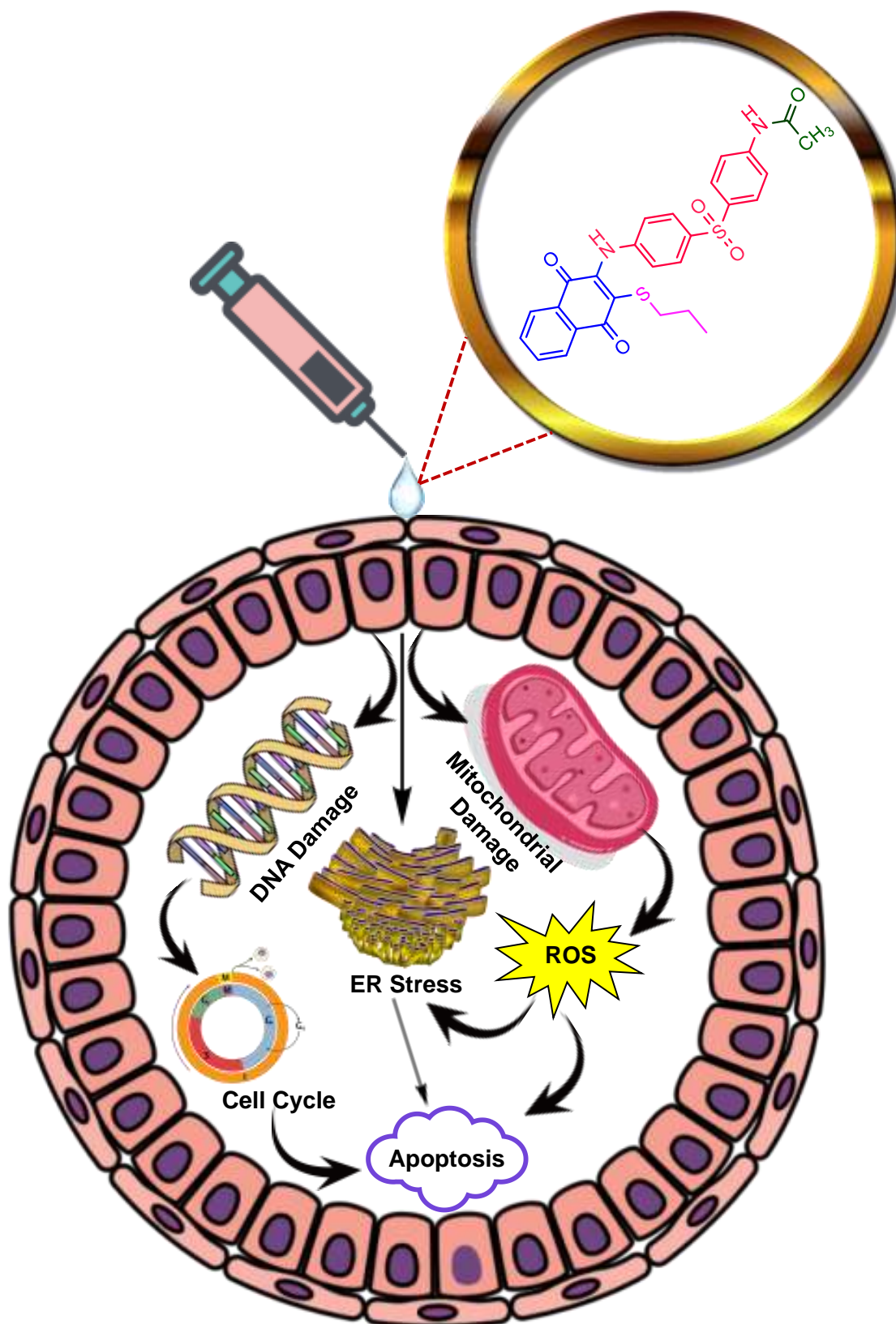


Fig. 12. Proposed mode of mechanism of action of 5v in cancer cells.

The current research emphasizes the advancement of novel anticancer agents and the assessment of their efficacy in animal models; however, there remain significant opportunities within the same library of molecules to create anticancer agents that are more appropriate for clinical trials.

3.4. *In silico analysis*

ER receptors mediate estrogen was selected as study model, which is involved in several physiological functions such as growth, development, and homeostasis in several tissues. Doxorubicin is widely used to treat ER+ breast cancer that inhibits DNA by intercalating and inhibiting macromolecular biosynthesis. The obtained docking results indicate that the ER α -binding site was identified as a relatively large portion of the ligand-binding domain hydrophobic core. It is mainly located on Met342 to Leu354, Trp383 to Arg 394, and the loop region Val418 to Leu428, Met 517 to Met528, and the hairpin Leu402 to Leu 410. Here, we docked **5v** against the ER receptors and used doxorubicin as reference to determine the differences in binding interactions. The binding sites for doxorubicin consisted of four hydrogen bonds (Fig. S2a), whereas **5v** bound to both chains and showed 22 hydrogen bonds at a distance of 0.5 nm. Hydrogen bonds and π -alkyl interactions with Lys520 were also observed at **5v** binding site. Furthermore, **5v** exhibited hydrophobic interactions with several residues, which increased the binding energy (Fig. 13a and Table S2). **5v** binding pocket exhibited greater depth and strength compared to that of doxorubicin due to the robust interactions among the receptor chains.

Additionally, the epidermal growth factor receptor (EGFR) stands out as a key target receptor in breast cancer. These transmembrane proteins become activated upon binding with epidermal growth factor and transforming growth factor- α . Mutations and misregulation of EFGR result in uncontrolled cell growth and cancers, including lung, intestinal, and breast cancers. Doxorubicin binds tightly to the EFGR receptor surface; however, **5v** occupies the

deep cavity of the receptor. The binding site of doxorubicin was found to have 12 hydrogen bonds with residues. In addition to hydrogen bonds, Lys875, Ala722, Glu758, Pro877, and Val876 showed hydrophobic interactions with doxorubicin (Fig. S2b). In contrast, **5v** exhibits a higher number of hydrogen bonds and a hydrophobic cavity at the binding site (Fig. 13b and Table S2). The presence of a hydrophobic pocket increases the affinity of **5v** for EGFR. Compounds that target EGFR hinder cell growth by halting the cell cycle and inducing apoptosis, while breast cancer type 1 susceptibility proteins play a role in repairing DNA damage.

The BRCA1 receptor showed a hydrogen-bonding pattern similar to that of both doxorubicin and **5v** (Figs 13c & S2c). It was also noted that the docking binding scores were found to be similar, indicating that **5v** may not a potential target for BRCA1. BRCA1 repairs double-stranded DNA breaks, thereby increasing cell multiplication. Hence, it is widely inhibited in cancer treatment along with other chemotherapeutic agents. Here, VEGFR2 showed a strong affinity for **5v**. As shown in Table S2, the highest number of interacting residues was observed for VEGFR2, indicating a potential inhibitory action of **5v**. Furthermore, the alignment of **5v** with DNA (Fig. 13d) occupied more space in the DNA pair interactions than doxorubicin (Fig. S1a, b). **5v** appears to break interpair interactions by occupying the base pair and causing structural changes. Furthermore, **5v** exhibited superior docking scores (-9.1, -7.1, -8.9, and -10.9 kcal/mol) compared to doxorubicin (-7.2, -6.1, -6.9, and -7.3 kcal/mol) against ER, EGFR, BRCA1, and VEGFR2 receptors, respectively.

The ADMET profile of compound **5v** shows high oral absorption (60%), with higher intestine absorption (95%) (Table S3). **5v** shows a wide range of activity against cytochrome P450 enzymes, except for 2D6; hence, further curation of the liver enzyme is required. Apart from the cytochrome P450 enzymes, the crucial efflux receptor/enzyme interactions were less, and the drug molecule showed moderate aqueous solubility and lipophilicity. Besides, the

toxicities of **5v** and doxorubicin were compared using a protox webserver.^[77] The LD₅₀ value for doxorubicin was found to be 20 mg/kg, and that of the drug molecule **5v** was 200 mg/kg which classified as a less toxic class 4 substance, whereas doxorubicin was classified as class 3. *In vitro* and *in vivo* toxicity evaluations also showed inactive toxicity in all vital organs, including the kidneys, and heart.

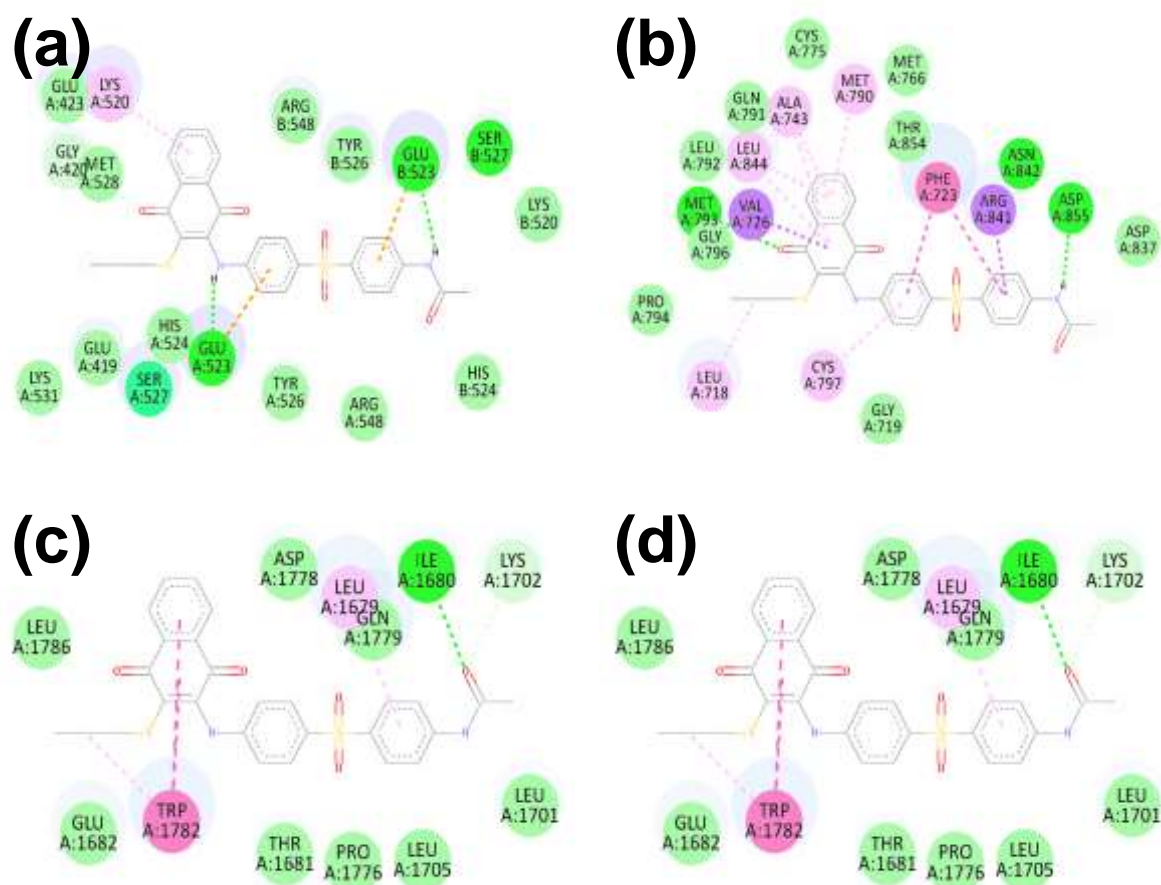


Fig. 13. (a–d) The interaction between the **5v** and the surrounding residues of the receptors ER, EFGR, BRCA1 and VEFGR2, respectively.

4. Conclusions

Naphthoquinones, a class of biologically active molecules, are extensively utilized as drugs for cancer, malarial, bacterial, and fungal treatment. Despite their widespread use, there has been a lack of research on combining the 1,4-naphthoquinone scaffold with an amide and aliphatic long chains with heteroatom fragment for use as an anticancer agent. In this particular

investigation, a series of new anticancer agents with the ability to induce ROS and bearing a core structure of 1,4-dioxo-3-(propylthio)-1,4-dihydronaphthalen-2-yl)amino)phenyl)sulfonyl)phenyl have been designed, synthesized, and evaluated for their anticancer activity and selectivity. Amongst, the most active compound **5v** exhibits broad-spectrum antitumor activity, particularly against MCF-7 breast cancer cell line ($IC_{50} = 1.2 \mu\text{M}$ and $0.9 \mu\text{M}$ at 24 hours and 48 hours, respectively) compared to the standard drug doxorubicin ($IC_{50} = 2.4 \mu\text{M}$ and $2.1 \mu\text{M}$ at 24 hours and 48 hours, respectively). Moreover, it demonstrates good selectivity between MCF-7 breast cancer cells and HEK293 normal cells (with a selectivity ratio of more than 8-fold). Notably, remarkable anticancer property of **5v** was confirmed by various analysis such as cell morphological changes, AO/EB double staining, apoptosis analysis, cell colony formation assay, SDS-PAGE and Western blotting study, cell cycle analysis, and ROS assay. These studies indicate that the anticancer mechanism was operated *via* generating ROS, promoting apoptosis/necrosis, causing cell cycle arrest in the G1/S phase. Furthermore, *in vivo* xenotransplantation of MCF-7 cells in zebrafish larvae against **5v** confirmed a significant reduction in tumor volume in the xenograft. The ecotoxicity studies indicate that **5v** ($LC_{50} = 50.15 \mu\text{M}$) is safe to use in animal models. These findings highlight the effectiveness of integrating 1,4-naphthoquinone scaffold with an amides and aliphatic long chains with heteroatom fragment as a promising approach for developing new medicines with exceptional activity and safety. Impending studies will focus on evaluating these molecular scaffolds for their potential to inhibit the growth of various tumours in humans.

Supporting Information

Molecular docking studies of compound **5v**, and NMR spectra for compounds **3-5aa** are provided in the supporting information.

CRedit authorship contribution statement

P. Ravichandiran: Writing – review & editing, Writing – original draft, Investigation, Formal analysis, Data curation, Supervision, Project administration, Funding acquisition, Conceptualization. **A. Martyna, E. Kochanowicz:** Formal analysis, Data curation. **N. Maroli:** *In silico* studies. **K. Kubiński, M. Maslyk, A. Boguszewska-Czubara:** Formal analysis, Data curation, Funding acquisition. **T. Ramesh:** Formal analysis, Data curation.

Declaration of competing interest

The authors declare that they have no known competing financial interests or personal relationships that could have appeared to influence the work reported in this paper.

Acknowledgment

This work was partially supported by the Polish National Science Centre research grant (UMO-2019/33/B/NZ7/01608) for the studies to develop the experimental model of tumor cell xenografts *in vivo* with use of *Danio rerio* as model organism.

References

- [1] M. Agarwal, O. Afzal, Salahuddin, A. S. A. Altamimi, M. A. Alamri, M. A. Alossaimi, V. Sharma, M. J. Ahsan, *ACS Omega* **2023**, 8(30), 26837-26849.
- [2] A. S. de Souza, D. S. Dias, R. C. B. Ribeiro, D. C. S. Costa, M. G. de Moraes, D. R. Pinho, M. E. G. Masset, L. M. Marins, S. P. Valle, C. J. C. de Carvalho, G. S. G. de Carvalho, A. L. N. Mello, M. Sola-Penna, M. V. Palmeira-Mello, R. A. Conceição, C. R. Rodrigues, A. M. T. Souza, L. d. S. M. Forezi, P. Zancan, V. F. Ferreira, F. d. C. da Silva, *Bioorg. Med. Chem.* **2024**, 102, 117671.
- [3] H. Sung, J. Ferlay, R. L. Siegel, M. Laversanne, I. Soerjomataram, A. Jemal, F. Bray, *Ca-Cancer J. Clin.* **2021**, 71(3), 209-249.
- [4] R. L. Siegel, K. D. Miller, H. E. Fuchs, A. Jemal, **2022**, 72(1), 7-33.
- [5] <https://www.who.int/news-room/fact-sheets/detail/breast-cancer>, Accessed on 04/04/2024 **2024**.

- [6] K. Sathishkumar, M. Chaturvedi, P. Das, S. Stephen, P. Mathur, *Indian J. Med. Res.* **2022**, *156*(4&5), 598-607.
- [7] D. T. Debela, S. G. Muzazu, K. D. Heraro, M. T. Ndalama, B. W. Mesele, D. C. Haile, S. K. Kitui, T. Manyazewal, *SAGE Open Med.* **2021**, *9*, 20503121211034366.
- [8] S. Zargan, M. Salehi Barough, J. Zargan, M. Shayesteh, A. Haji Noor Mohammadi, M. Mousavi, H. Keshavarz Alikhani, *J. Appl. Biotechnol. Rep.* **2022**, *9*(1), 547-556.
- [9] X. Ji, Y. Lu, H. Tian, X. Meng, M. Wei, W. C. Cho, *Biomed. Pharmacother.* **2019**, *114*, 108800.
- [10] H.-Y. Qiu, P.-F. Wang, H.-Y. Lin, C.-Y. Tang, H.-L. Zhu, Y.-H. Yang, *Chem. Biol. Drug Des.* **2018**, *91*(3), 681-690.
- [11] F. de Carvalho da Silva, V. Francisco Ferreira, *Curr. Org. Synth.* **2016**, *13*(3), 334-371.
- [12] D. J. Newman, G. M. Cragg, *J. Nat. Prod.* **2020**, *83*(3), 770-803.
- [13] S. A. M. Khalifa, N. Elias, M. A. Farag, L. Chen, A. Saeed, M.-E. F. Hegazy, M. S. Moustafa, A. Abd El-Wahed, S. M. Al-Mousawi, S. G. Musharraf, F.-R. Chang, A. Iwasaki, K. Suenaga, M. Alajlani, U. Göransson, H. R. El-Seedi, *Mar. Drugs* **2019**, *17*(9), 491.
- [14] X. Ren, X. Xie, B. Chen, L. Liu, C. Jiang, Q. Qian, *J. Med. Chem.* **2021**, *64*(12), 7879-7899.
- [15] S. Dasari, S. Njiki, A. Mbemi, C. G. Yedjou, P. B. Tchounwou, *Int. J. Mol. Sci.* **2022**, *23*(3), 1532.
- [16] E. Angulo-Elizari, A. Henriquez-Figueroa, C. Morán-Serradilla, D. Plano, C. Sanmartín, *Eur. J. Med. Chem.* **2024**, *268*, 116249.
- [17] L. Zhu, K. Li, M. Liu, K. Liu, S. Ma, W. Cai, *Recent Pat. Anti-Cancer Drug Discovery* **2022**, *17*(3), 218-230.

- [18] A. A. Kamarudin, N. H. Sayuti, N. Saad, N. A. A. Razak, N. M. Esa, *Int. J. Mol. Sci.* **2021**, 22(13), 6747.
- [19] A. Mili, S. Das, K. Nandakumar, R. Lobo, *J. Ethnopharmacol.* **2021**, 281, 114503.
- [20] M. B. Martins-Teixeira, I. Carvalho, *ChemMedChem* **2020**, 15(11), 933-948.
- [21] P. S. Rawat, A. Jaiswal, A. Khurana, J. S. Bhatti, U. Navik, *Biomed. Pharmacother.* **2021**, 139, 111708.
- [22] A. Bhagat, E. S. Kleinerman, *Adv. Exp. Med. Biol.* **2020**, 1257, 181-192.
- [23] N. Brindani, F. Munafò, A. Menichetti, E. Donati, M. Nigro, G. Ottonello, A. Armirotti, M. De Vivo, *Bioorg. Med. Chem.* **2023**, 80, 117179.
- [24] T. Yao, X. Zeng, H. Li, T. Luo, X. Tao, H. Xu, *Int. J. Biol. Macromol.* **2024**, 269, 132115.
- [25] P. Ravichandiran, S. Sheet, D. Premnath, A. R. Kim, D. J. Yoo, 1,4-Naphthoquinone analogues: Potent antibacterial agents and mode of action evaluation, in *Molecules*, Vol. 24, **2019**.
- [26] N. S. Mone, S. Syed, P. Ravichandiran, E. E. Kamble, K. R. Pardesi, S. Salunke-Gawali, M. Rai, A. Vikram Singh, S. Prasad Dakua, B.-H. Park, D. J. Yoo, S. K. Satpute, *ChemMedChem* **2023**, 18(24), e202300328.
- [27] G. C. Brandão, F. C. Rocha Missias, L. M. Arantes, L. F. Soares, K. K. Roy, R. J. Doerksen, A. Braga de Oliveira, G. R. Pereira, *Eur. J. Med. Chem.* **2018**, 145, 191-205.
- [28] L. Salmon-Chemin, E. Buisine, V. Yardley, S. Kohler, M.-A. Debreu, V. Landry, C. Sergheraert, S. L. Croft, R. L. Krauth-Siegel, E. Davioud-Charvet, *J. Med. Chem.* **2001**, 44(4), 548-565.
- [29] P. Ravichandiran, A. Jegan, D. Premnath, V. S. Periasamy, S. Muthusubramanian, S. Vasanthkumar, *Bioorg. Chem.* **2014**, 53, 24-36.
- [30] P. Ravichandiran, A. Jegan, D. Premnath, V. S. Periasamy, S. Vasanthkumar, *Med. Chem. Res.* **2015**, 24(1), 197-208.

- [31] Q. Cui, C. Huang, J.-Y. Liu, J.-T. Zhang, *J. Med. Chem.* **2023**, *66*(24), 16515-16545.
- [32] J. Yuan, Z. Liu, Y. Dong, F. Gao, X. Xia, P. Wang, Y. Luo, Z. Zhang, D. Yan, W. Zhang, *J. Med. Chem.* **2023**, *66*(24), 16843-16868.
- [33] M. M. Rahman, M. R. Islam, S. Akash, S. Shohag, L. Ahmed, F. A. Supti, A. Rauf, A. S. M. Aljohani, W. Al Abdulmonem, A. A. Khalil, R. Sharma, M. Thiruvengadam, *Chem.-Biol. Interact.* **2022**, *368*, 110198.
- [34] J. Maneenet, N. Tajuddeen, H. Hong Nguyen, R. Fujii, B. Kimbadi Lombe, D. Feineis, S. Awale, G. Bringmann, *Results Chem.* **2024**, *7*, 101352.
- [35] K. Ali, P. Mishra, A. Kumar, D. N. Reddy, S. Chowdhury, G. Panda, *Chem. Commun* **2022**, *58*(42), 6160-6175.
- [36] N. Soonthornchareonnon, K. Suwanborirux, R. Bavovada, C. Patarapanich, J. M. Cassady, *J. Nat. Prod.* **1999**, *62*(10), 1390-1394.
- [37] L. F. Fieser, E. Berliner, F. J. Bondhus, F. C. Chang, W. G. Dauben, M. G. Ettliger, G. Fawaz, M. Fields, M. Fieser, C. Heidelberger, H. Heymann, A. M. Seligman, W. R. Vaughan, A. G. Wilson, E. Wilson, M.-i. Wu, M. T. Leffler, K. E. Hamlin, R. J. Hathaway, E. J. Matson, E. E. Moore, M. B. Moore, R. T. Rapala, H. E. Zaugg, *J. Am. Chem. Soc.* **1948**, *70*(10), 3151-3155.
- [38] J. A. Valderrama, M. Cabrera, J. Benites, D. Ríos, R. Inostroza-Rivera, G. G. Muccioli, P. B. Calderon, *RSC Adv.* **2017**, *7*(40), 24813-24821.
- [39] R. M. Costa Souza, L. M. L. Montenegro Pimentel, L. K. M. Ferreira, V. R. A. Pereira, A. C. D. S. Santos, W. M. Dantas, C. J. O. Silva, R. M. De Medeiros Brito, J. L. Andrade, V. F. De Andrade-Neto, R. T. Fujiwara, L. L. Bueno, V. A. Silva Junior, L. Pena, C. A. Camara, B. Rathi, R. N. De Oliveira, *Eur. J. Med. Chem.* **2023**, *255*, 115400.
- [40] J. Benites, J. A. Valderrama, K. Bettega, R. C. Pedrosa, P. B. Calderon, J. Verrax, *Eur. J. Med. Chem.* **2010**, *45*(12), 6052-6057.

- [41] B. Devi Bala, S. Muthusarayanan, T. S. Choon, M. Ashraf Ali, S. Perumal, *Eur. J. Med. Chem.* **2014**, *85*, 737-746.
- [42] V. Prachayasittikul, R. Pingaew, A. Worachartcheewan, C. Nantasenamat, S. Prachayasittikul, S. Ruchirawat, V. Prachayasittikul, *Eur. J. Med. Chem.* **2014**, *84*, 247-263.
- [43] R. Pingaew, V. Prachayasittikul, A. Worachartcheewan, C. Nantasenamat, S. Prachayasittikul, S. Ruchirawat, V. Prachayasittikul, *Eur. J. Med. Chem.* **2015**, *103*, 446-459.
- [44] H. Yıldırım, N. Bayrak, A. F. Tuyen, E. M. Kara, B. Ö. Çelik, G. K. Gupta, *RSC Adv.* **2017**, *7*(41), 25753-25764.
- [45] J. S. Novais, C. S. Moreira, A. C. J. A. Silva, R. S. Loureiro, A. M. Sá Figueiredo, V. F. Ferreira, H. C. Castro, D. R. da Rocha, *Microb. Pathog.* **2018**, *118*, 105-114.
- [46] P. Ravichandiran, M. Maslyk, S. Sheet, M. Janeczko, D. Premnath, A. R. Kim, B.-H. Park, M.-K. Han, D. J. Yoo, *ChemistryOpen* **2019**, *8*(5), 589-600.
- [47] P. Ravichandiran, J. Athinarayanan, D. Premnath, V. S. Periasamy, A. A. Alshatwi, S. Vasanthkumar, *Spectrochim. Acta, Part A* **2015**, *139*, 477-487.
- [48] N. S. Mone, S. Syed, P. Ravichandiran, S. K. Satpute, A. R. Kim, D. J. Yoo, *ChemMedChem* **2023**, *18*(2), e202200471.
- [49] P. Ravichandiran, R. Kannan, A. Ramasubbu, S. Muthusubramanian, V. K. Samuel, *J. Saudi Chem. Soc.* **2016**, *20*, S93-S99.
- [50] H. Becker, W. Berger, G. Domschke, E. Fanghänel, J. Faust, M. Fischer, F. Gentz, K. Gewalt, R. Gluch, R. Mayer, K. Müller, D. Pavel, H. Schmidt, K. Schollberg, K. Schwetlick, G. Zeppenfeld, in *Organicum* (Eds.: H. Becker, W. Berger, G. Domschke, E. Fanghänel, J. Faust, M. Fischer, F. Gentz, K. Gewalt, R. Gluch, R. Mayer, K. Müller,

- D. Pavel, H. Schmidt, K. Schollberg, K. Schwetlick, G. Zeppenfeld), Pergamon, **1973**, pp. 607-664.
- [51] K. Brand, K. Trebing, *Berichte der deutschen chemischen Gesellschaft (A and B Series)* **1923**, 56(11), 2545-2547.
- [52] *Proc. Chem. Soc.* **1962**(June), 197-236.
- [53] B. Deka, T. Sarkar, A. Bhattacharyya, R. J. Butcher, S. Banerjee, S. Deka, K. K. Saikia, A. Hussain, *Dalton Trans.* **2024**, 53(11), 4952-4961.
- [54] S. Yousuf, F. Arjmand, S. Tabassum, *Polyhedron* **2021**, 209, 115450.
- [55] L. Wang, Y. Qian, *Org. Biomol. Chem.* **2023**, 21(36), 7339-7350.
- [56] G. Li, J.-Q. Wu, X. Cai, W. Guan, Z. Zeng, Y. Ou, X. Wu, J. Li, X. Fang, J. Liu, Y. Zhang, H. Wang, C. Yin, H. Yao, *Eur. J. Med. Chem.* **2023**, 252, 115284.
- [57] N. Kohyanagi, N. Kitamura, S. Ikeda, S. Shibutani, K. Sato, T. Ohama, *J. Biol. Chem.* **2024**, 300(1), 105584.
- [58] A. Valsan, M. T. Meenu, V. P. Murali, B. Malgija, A. G. Joseph, P. Nisha, K. V. Radhakrishnan, K. K. Maiti, *ACS Omega* **2023**, 8(16), 14799-14813.
- [59] S. A. Abdel-Rahman, A. K. El-Damasy, G. S. Hassan, E. I. Wafa, S. M. Geary, A. R. Maarouf, A. K. Salem, *ACS Pharmacol. Transl. Sci.* **2020**, 3(5), 965-977.
- [60] J. Haribabu, R. Arulkumar, D. Mahendiran, K. Jeyalakshmi, S. Swaminathan, P. Venuvanalingam, N. Bhuvanesh, J. F. Santibanez, R. Karvembu, *Inorg. Chim. Acta* **2024**, 565, 121973.
- [61] P. Ravichandiran, D. S. Prabakaran, N. Maroli, A. Boguszewska-Czubara, M. Maslyk, A. R. Kim, P. Kolandaivel, P. Ramalingam, B.-H. Park, M.-K. Han, T. Ramesh, D. J. Yoo, *J. Hazard. Mater.* **2021**, 415, 125593.

- [62] S. Kuttikrishnan, M. Hasan, K. S. Prabhu, T. El-Elimat, N. H. Oberlies, C. J. Pearce, F. Q. Alali, A. Ahmad, E. Pourkarimi, A. A. Bhat, H. C. Yalcin, S. Uddin, *Exp. Cell Res.* **2024**, *435*(1), 113907.
- [63] A. Kocere, J. Resseguier, J. Wohlmann, F. M. Skjeldal, S. Khan, M. Speth, N.-J. K. Dal, M. Y. W. Ng, N. Alonso-Rodriguez, E. Scarpa, L. Rizzello, G. Battaglia, G. Griffiths, F. Fenaroli, *EBioMedicine* **2020**, *58*, 102902.
- [64] O. Trott, A. J. Olson, *J. Comput. Chem.* **2010**, *31*(2), 455-461.
- [65] R. Boddiboyena, G. Sridhar, G. N. Reddy, N. Seelam, M. Sarma, D. Kolli, M. R. Gudisela, *Results Chem.* **2024**, *7*, 101334.
- [66] H. Yang, C. Lou, L. Sun, J. Li, Y. Cai, Z. Wang, W. Li, G. Liu, Y. Tang, *Bioinformatics* **2019**, *35*(6), 1067-1069.
- [67] P. Ravichandiran, S. A. Subramaniyan, S.-Y. Kim, J.-S. Kim, B.-H. Park, K. S. Shim, D. J. Yoo, *ChemMedChem* **2019**, *14*(5), 532-544.
- [68] M. A. Sabry, M. A. Ghaly, A. R. Maarouf, H. I. El-Subbagh, *Eur. J. Med. Chem.* **2022**, *241*, 114661.
- [69] K. Gholivand, M. Faraghi, M. Vahabirad, R. E. Malekshah, S. Narimani, R. Roohzadeh, N. Fallah, S. Jannesar, M. Yousefian, *J. Mol. Struct.* **2025**, *1319*, 139167.
- [70] R. I. Nicholson, J. M. W. Gee, M. E. Harper, *Eur. J. Cancer* **2001**, *37*, 9-15.
- [71] M. V. Raimondi, O. Randazzo, M. La Franca, G. Barone, E. Vignoni, D. Rossi, S. Collina, DHFR inhibitors: Reading the past for discovering novel anticancer agents, in *Molecules*, Vol. 24, **2019**.
- [72] D. Amujuri, B. Siva, B. Poornima, K. Sirisha, A. V. S. Sarma, V. Lakshma Nayak, A. K. Tiwari, U. Purushotham, K. Suresh Babu, *Eur. J. Med. Chem.* **2018**, *149*, 182-192.

- [73] N. M. Vinita, U. Devan, S. Durgadevi, S. Anitha, M. Govarthan, A. Antony Joseph Velanganni, J. Jeyakanthan, P. Arul Prakash, M. S. Mohamed Jaabir, P. Kumar, *ACS Omega* **2023**, 8(37), 33229-33241.
- [74] Y.-L. Li, X.-M. Zhu, N.-F. Chen, S.-T. Chen, Y. Yang, H. Liang, Z.-F. Chen, *Eur. J. Med. Chem.* **2022**, 236, 114312.
- [75] E. S. Al-Sheddi, N. Alsohaibani, N. bin Rshoud, M. M. Al-Oqail, S. M. Al-Massarani, N. N. Farshori, T. Malik, A. A. Al-Khedhairy, M. A. Siddiqui, *S. Afr. J. Bot.* **2023**, 160, 123-131.
- [76] J. M. Mendonça-Gomes, T. M. Valverde, T. M. d. M. Martins, I. Charlie-Silva, B. N. Padovani, C. M. Fénero, E. M. da Silva, R. Z. Domingues, D. C. Melo-Hoyos, J. D. Corrêa-Junior, N. O. S. Câmara, A. M. Góes, D. A. Gomes, *Fish Shellfish Immunol.* **2021**, 2, 100007.
- [77] P. Banerjee, A. O. Eckert, A. K. Schrey, R. Preissner, *Nucleic Acids Res.* **2018**, 46(W1), W257-W263.